Preserved extensional structures in an inverted Cretaceous rift basin, northwestern Argentina: Outcrop examples and implications for fault reactivation

César R. Monaldi,[1] José A. Salfity,[1] and Jonas Kley[2]

Received 16 May 2006; revised 5 October 2007; accepted 26 October 2007; published 14 February 2008.

[1] During the Cretaceous-Eocene interval a system of intracontinental rift basins, the Salta group rift, evolved in northwestern Argentina. Individual segments of the rift later suffered different degrees of inversion during Cenozoic shortening. The Tres Cruces subbasin, on the west side of the Eastern Cordillera, was strongly deformed, being now part of a thick-skinned thrust belt with a predominantly N-S structural trend. On its eastern border, tilting due to folding and thrusting and subsequent erosion have produced exceptional outcrops of preserved east-trending extensional structures including half grabens, rollover anticlines, and extensional fault-propagation folds. Farther west, the synrift succession is only intermittently exposed, although the interference of north- and east-trending structures as well as peculiar, dome-shaped anticlines with spur-like extensions suggest that north- and east-trending Cretaceous faults were reactivated, particularly near their intersections. Compilation of published data and analysis of our new data focused on the Salta rift indicates three main factors favoring the contractional reactivation of normal faults: dip angles lower than approximately 60°, especially for faults striking roughly normal to contraction; strikes no closer to the contraction direction than approximately 30°; and low downdip fault curvatures. Occasional dip-slip reactivation of east-trending faults does not match the present and long-term Andean stress regimes and presents an unresolved problem. **Citation:** Monaldi, C. R., J. A. Salfity, and J. Kley (2008), Preserved extensional structures in an inverted Cretaceous rift basin, northwestern Argentina: Outcrop examples and implications for fault reactivation, *Tectonics*, *27*, TC1011, doi:10.1029/2006TC001993.

1. Introduction

[2] Between Late Jurassic and Eocene times, northwestern Argentina, southern Paraguay and Bolivia, and northeastern Chile were affected by extensional processes that resulted in the formation of an intracontinental rift (Figure 1) which was filled by sedimentary series as thick as 5500 m, intercalated with a minor volume of magmatic rocks. This complex constitutes the Salta group [*Galliski and Viramonte*, 1988; *Salfity and Marquillas*, 1994; *Marquillas et al.*, 2005]. The closure of the extensional basin began approximately at the end of the Eocene [*Salfity et al.*, 1993; *Coutand et al.*, 2001; *Hongn et al.*, 2007] because of compressive processes linked to the subduction of the Farallones plate under the South American plate [*Pardo-Casas and Molnar*, 1987]. This provoked a rapid transition from a rift basin to a foreland basin filled by synorogenic continental deposits. Contractional deformation of the rift basin is diachronous, with the main phase of contraction ranging from Eocene [*Hongn et al.*, 2007] over Oligocene [*Carrapa et al.*, 2005] in the western region to late Miocene or Pliocene time [*Reynolds et al.*, 2000; *Kley and Monaldi*, 2002] in the east.

[3] The first mentions of normal faults controlling the thicknesses of the Salta group are found in unpublished reports (T. H. Hagerman, La geología de las serranías Santa Bárbara, Cachipunco, Centinela, La Ronda y Maíz Gordo, en las provincias de Salta y Jujuy y las relaciones petrolíferas de la zona, unpublished report, 1932; A. Russo, Levantamiento geológico de la parte del río Iruya, entre sus cabeceras y el río Astilleros, unpublished report, 1949) of Yacimientos Petrolíferos Fiscales, the formerly state-owned Argentine hydrocarbon exploration company. Later stratigraphic and structural analyses on a basin-wide scale revealed that the Salta group was deposited in a rift basin which had suffered different degrees of inversion during the Cenozoic Andean orogeny [i.e., *Bianucci and Homovc*, 1982; *Bianucci et al.*, 1982; *Uliana and Biddle*, 1988; *Grier*, 1990; *Grier et al.*, 1991; *Kress*, 1995; *Comínguez and Ramos*, 1995; *Uliana et al.*, 1995; *Cristallini et al.*, 1997; *Bianucci*, 1999; *Kley and Monaldi*, 2002].

[4] Despite the well-established general structure of the Salta rift basin, documented examples of Cretaceous normal faults are rare and most refer to faults reactivated as reverse faults [*Grier et al.*, 1991; *Salfity and Marquillas*, 1994; *Gangui and Götze*, 1996; *Gangui*, 1998; *Kley et al.*, 2005; *Carrera et al.*, 2006]. As far as we know, only two examples of at least partially preserved normal faults have been reported [*Kley et al.*, 2005; *Carrera et al.*, 2006]. In this paper we present a case study of exposed extensional faults that have demonstrably not suffered any major modification or reactivation. The most conspicuous structure is a large listric normal fault with a well-developed half-graben fill and rollover anticline. This association is a

[1]Consejo Nacional de Investigaciones Científicas y Técnicas, Universidad Nacional de Salta, Salta, Argentina.
[2]Institut für Geowissenschaften, Friedrich-Schiller-Universität Jena, Jena, Germany.

0278-7407/08/2006TC001993$12.00

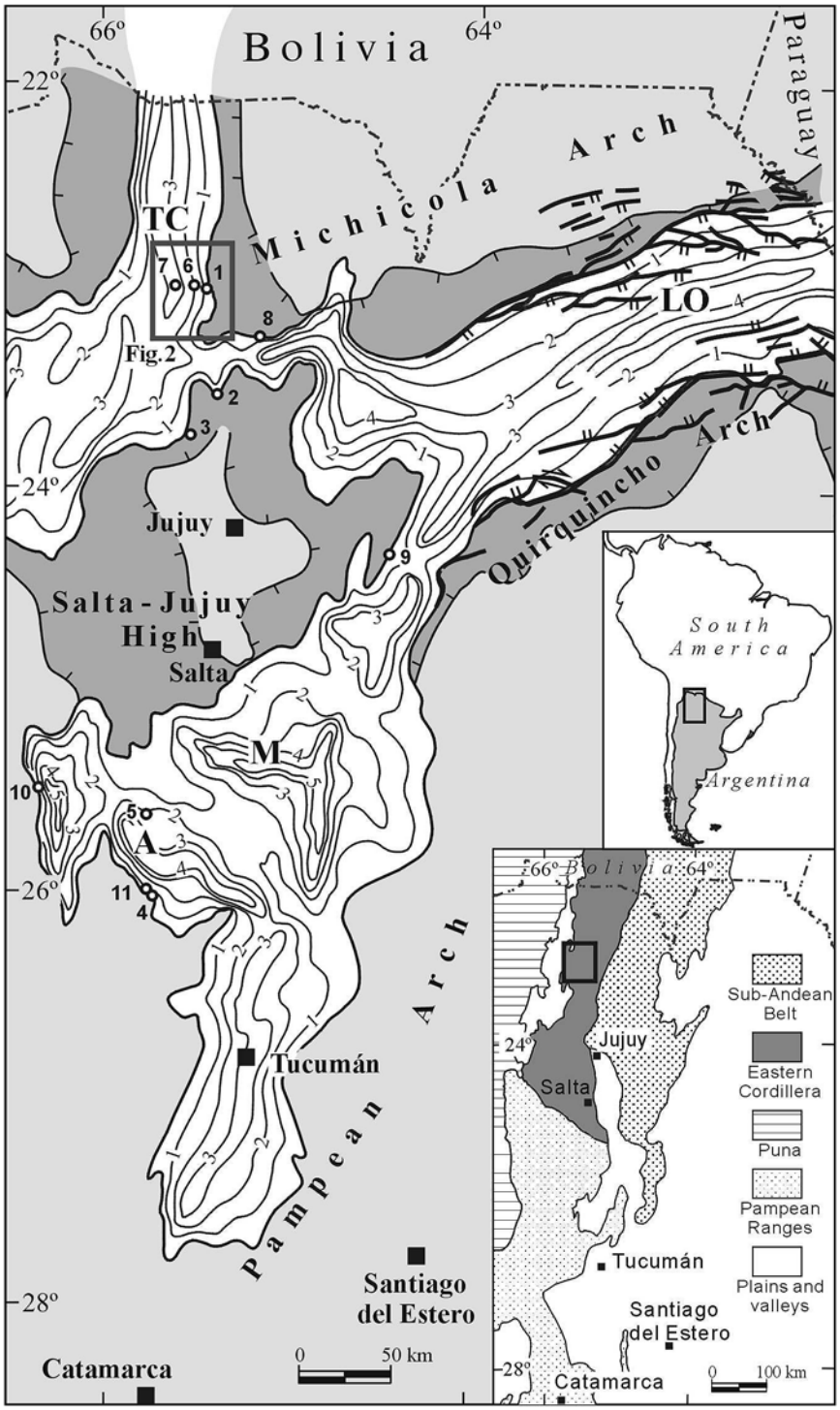

Figure 1. Overview map of the Salta group rift (modified from *Salfity and Marquillas* [1994]). The main subbasins are A, Alemania; LO, Lomas de Olmedo; M, Metán; TC, Tres Cruces. Blank areas correspond to synrift deposits, with isopachs in km; dark grey denotes extent of postrift deposits and light grey denotes syndepositional highs. Small open circles with numbers 1–11 indicate the locations of faults listed in Table 1. The rectangle indicates the location of Figure 2. Upper inset shows the location of Figure 1. Lower inset shows the location of Figure 2 with respect to the geological provinces of northern Argentina.

basic element of many structural models in extensional areas [e.g., *Dula*, 1991] and has often been documented in seismic data, although exposed examples are scarce. We discuss similarities and differences of our case study with respect to the ideal listric fault model. We then use the evidence from both preserved and reactivated normal faults to constrain the conditions for reverse reactivation of extensional faults in the Salta rift.

2. Geologic Setting

[5] The region analyzed in the present work is located on the western border of the Eastern Cordillera in the area bordering the Puna plateau. The Eastern Cordillera is a high-standing mountain chain (regional peak elevation in Cerro Chañi is 6200 m above sea level) that forms the eastern margin of the high Andes in northern Argentina. It lies between the Puna plateau in the west and the sub-Andean ranges/Santa Bárbara system foothills in the east (Figure 1, inset). The Eastern Cordillera exhibits a typical thick-skinned thrust belt structural style. Its structure is marked by imbricated thrust sheets that often expose the Proterozoic basement and, to a lesser extent, by folds bounded by reverse or thrust faults. The faults and folds trend N-S, with slight deviations toward the northwest and northeast. The faults dip steeply near the surface but flatten at depth as can be observed on seismic lines [*Gangui*, 1998; *Coutand et al.*, 2001; *Kley et al.*, 2005]. In the segment discussed here the dominant vergence is to the east, although backthrusts with opposite vergence are also observed (Figure 2).

[6] The oldest rocks exposed in the study area (Figures 2 and 3) are marine slates and sandstones of the Puncoviscana formation (Upper Proterozoic to Lower Cambrian) that were strongly folded, slightly metamorphosed, and intruded by granites in Middle Cambrian time. The Puncoviscana formation is overlain in angular unconformity by quartzites and marine sandstones of the Mesón group (Upper Cambrian), separated in turn by a regional unconformity from the marine shales and sandstones of the Santa Victoria group (Lower Ordovician). Shortly before the onset of rifting and related redbed deposition in Cretaceous time, several alkaline and subalkaline anorogenic plutons with Rb/Sr ages between 152 ± 2 and 110 ± 5 Ma [*Halpern and Latorre*, 1973; *Menegatti et al.*, 1997; *Viramonte et al.*, 1999] had intruded Paleozoic units. Two of these bodies, the Aguilar and Abra Laite stocks, are located on the southwestern margin of the area considered in this paper (Figure 2). The sedimentary rift fill corresponding to the Cretaceous to Eocene Salta group rests in slightly angular unconformity on Cambrian and Ordovician rocks.

[7] The Salta group, stratigraphic focus of this paper, is traditionally subdivided into three subgroups, which, from base to top, are termed the Pirgua, Balbuena, and Santa Bárbara subgroups [*Moreno*, 1970; *Reyes and Salfity*, 1973].The Pirgua subgroup, deposited in the synrift stage, consists of reddish conglomerates, sandstones, and shales from alluvial fan, fluvial, eolian, and lacustrine environments, with rare intercalations of volcanic rocks (basalts and trachytes [*Coira*, 1979]). In the Alemania subbasin (Figure 1) the Pirgua subgroup has been subdivided from bottom to top into the La Yesera, Las Curtiembres, and Los Blanquitos formations. However, this subdivision has not been extrapolated to the other subbasins owing to the strong lithostratigraphic variations presumably induced by local extensional faulting.

[8] The Balbuena and Santa Bárbara subgroups accumulated during the postrift stage. As they maintain their lithologic characteristics on a regional scale with no major variations, their correlations are relatively simple. The Balbuena subgroup comprises, from base to top, the Lecho and Yacoraite formations. These deposits accumulated in fluvial, eolian, and lacustrine environments. The Yacoraite formation, composed of light grey and yellow limestone, is an easily identifiable regional marker for structural mapping both in the field and on aerial photographs or satellite images. The Santa Bárbara subgroup consists of red and green pelite and sandstone deposited in fluvial and lacustrine environments. It is also subdivided into three formations, termed from base to top Mealla, Maíz Gordo, and Lumbrera.

[9] In a more recent study utilizing sequence stratigraphic techniques, the Salta group was subdivided into four supersequences: Pirgua, Balbuena, Santa Bárbara, and Lumbrera [*Hernández et al.*, 1999]. This subdivision is in general correlated one to one to the traditional lithostratigraphic units described above. The rift deposits are overlain by a thick coarsening upward succession of mudstones, sandstones and conglomerates that accumulated in a foreland basin in middle Eocene to Pliocene times (Casa Grande, Río Grande, and Pisungo formations).

3. Tres Cruces Synclinorium

3.1. Location in the Salta Rift

[10] According to available surface and subsurface data, the Salta rift has a general triradiate configuration around a central high (the Salta-Jujuy high or horst; Figure 1). The synrift basins, whose infill attains maximum thicknesses of more than 5000 m, are in many places overstepped by the latest Cretaceous to Paleogene sag sequence (Figure 1) [*Salfity and Marquillas*, 1994; *Marquillas et al.*, 2005]. The three partially or fully interconnected branches of the Salta rift have been described as individual subbasins, with the northern branch being termed Tres Cruces. The Tres Cruces subbasin has a north-trending axis and continues into Bolivia (the "Andean basin" of *Reyes* [1972]). Its prerift substrate is composed of Lower Paleozoic rocks (Cambrian and Ordovician). The eastern part of the basin is very well exposed, whereas its western part is almost completely covered by Neogene ignimbrite sheets and extensive Quaternary salt pans. There strata of the Tres Cruces subbasin strata only crop out discontinuously along thrust sheets, precluding a precise definition of its border. The eastern part of the Tres Cruces subbasin, deformed by Cenozoic folding and thrusting, constitutes the Tres Cruces synclinorium [*Boll and Hernández*, 1986; *Coutand et al.*, 2001; *Kley et al.*, 2005]. The strong contractional deforma-

Figure 2. Geological map of the Tres Cruces area, after *Méndez* [1973], *Kley et al.* [2005], and own observations. The locations of Figures 4 and 10 are indicated. ALS, Abra Laite stock; AS, Aguilar stock; CC, Cerro Colorado; CQ, Cerro Queñoal; EB, Esquinas Blancas; ED, Espinazo del Diablo; NMF, Negra Muerta fault; OHG, Ovara half graben; QF, Queñoal fault; SHG, Sapagua half graben; VBNF, Vicuñayoc-Barro Negro fault; 1, Quaternary; 2, Tertiary; 3, Santa Bárbara subgroup; 4, Balbuena subgroup; 5, Pirgua subgroup; 6, Cretaceous granitoids; 7, Ordovician; 8, Cambrian; 9, Precambrian; 10, anticline; 11, syncline; 12, thrust or reverse fault; 13, normal fault; 14, reactivated normal fault; 15, stream.

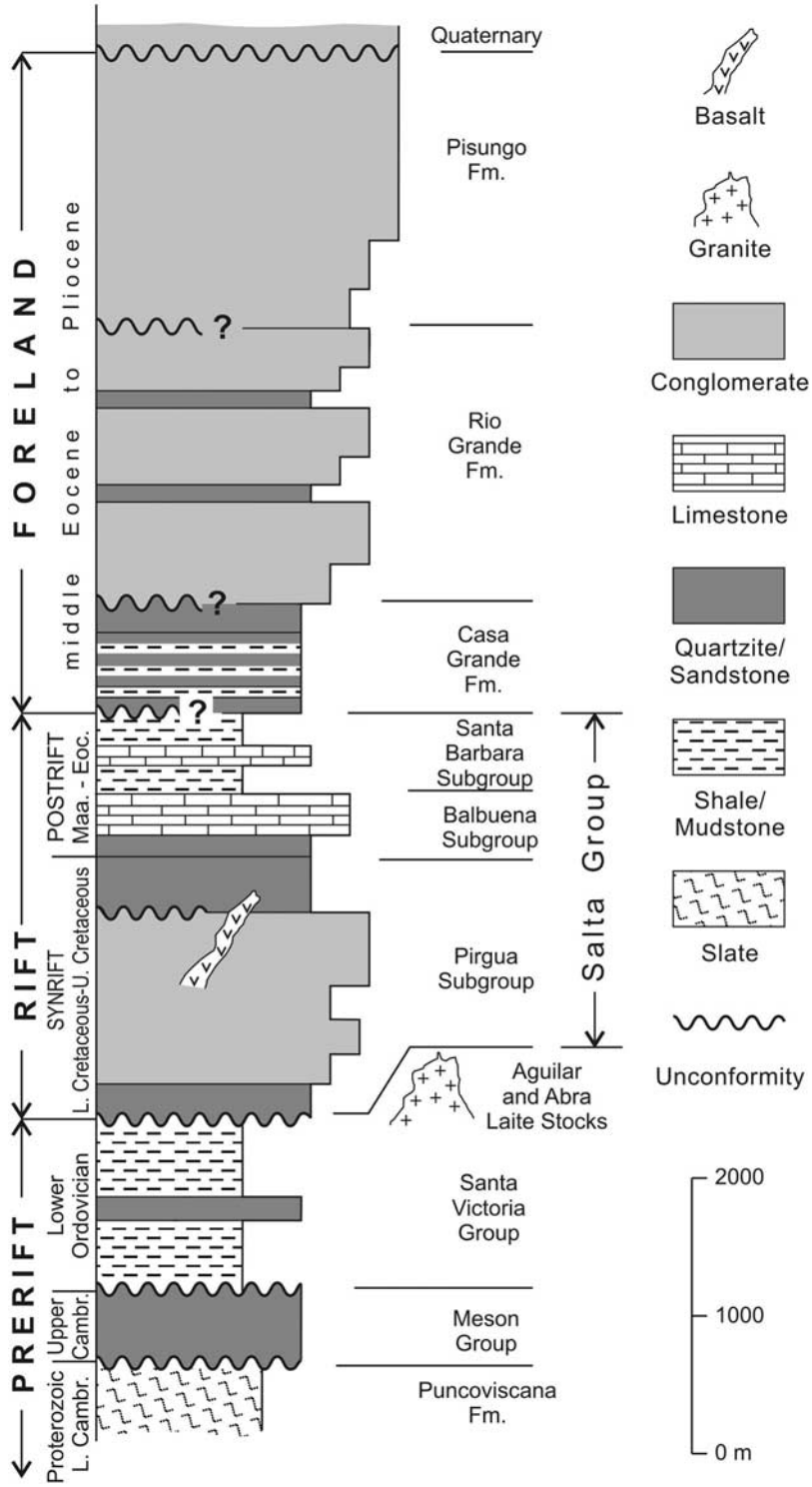

Figure 3. Stratigraphic column of the Tres Cruces area (modified after *Boll and Hernández* [1986]).

tion has largely masked the original rift architecture, which is why only a few normal faults can be recognized; and some reverse faults appear to be reactivated normal faults according to synrift thickness variations across strike.

3.2. Structure

[11] Compared to other areas located on the western border of the Eastern Cordillera, the Tres Cruces synclinorium is notable for its structural complexity resulting from the interference of crosscutting fault and fold trends (Figure 2). In order to simplify the description the area was separated into western, central, and eastern sectors, a subdivision previously proposed by *Méndez* [1973] and *Boll and Hernández* [1986].

3.2.1. Western Sector

[12] This area comprises the approximately 60 km long north-trending Sierra de Aguilar anticline, eroded at the level of Ordovician sedimentary rocks which host Early Cretaceous intrusive granitic bodies (the Aguilar and Abra Laite stocks). The eastern flank of the anticline is cut by a reverse fault that dips about 60° to the west [*Méndez*, 1973] whose fault trace is covered by Quaternary deposits along most of its length. Where the fault is exposed, Ordovician rocks are thrust over Tertiary strata or Cretaceous units.

3.2.2. Central Sector

[13] The central sector is a topographic depression almost completely covered by Quaternary deposits with some outcrops of Cretaceous and Tertiary rocks. At its northern and southern terminations the structural and topographic reliefs increase because of the emergence of two plunging anticlines cored by Lower Paleozoic strata: the south-plunging Tres Cruces anticlinorium in the north and the north-plunging Cajas anticline in the south. Within the central sector three N-S trending zones can be distinguished: In the west a thrust sheet corresponding to the Vicuñayoc-Barro Negro fault [*Boll and Hernández*, 1986] is exposed. This fault is an east-verging thrust with a sinuous trace. In the southern continuation of the Vicuñayoc-Barro Negro sheet is the Cajas anticline which comprises Cambrian to Cretaceous rocks at surface. This north-trending anticline is doubly plunging and asymmetric, with the steep to overturned western flank bounded by a west-verging reverse fault. In the axis of the central sector and flanked by two synclinal lows, lies the Cerro Colorado anticline which in map view is sigmoidal shaped and segmented by an axial depression in the middle. Its northern part is relatively simple and narrow. Its southern part widens abruptly and is affected by secondary folds, forming a small anticlinorium. The Cerro Colorado structure continues toward the south in the Espinazo del Diablo thrust sheet, with a west-verging reverse fault (the ''central fault'' of *Méndez* [1973]). The area east of Cerro Colorado has the highest topographic relief and greatest structural complexity of the region. Here we observe marked interferences between folds and faults of different trends, combined with abrupt thickness changes in the Cretaceous synrift strata. Three structures delimited by transverse faults (oblique or perpendicular to the main N-S fault trend) can be identified. These are, from north to south, the Esquinas Blancas anticline, the Sapagua anticlinorium, and the Cerro Queñoal anticlinorium.

3.2.3. Eastern Sector

[14] This area is essentially constituted by Precambrian and Ordovician rocks, with minor participation of Cretaceous and Tertiary strata. The faults trend approximately N-S, forming imbricated fans and displaying both east and west vergence. Folds are subordinate and some are dissected by faults.

3.3. Preserved Cretaceous Extensional Structures

[15] The clearest outcrop examples of well-preserved Cretaceous rift structures occur on the eastern border of the central synclinorium. The complicated structural geometry of this area on a regional and local scale arises from the interference between folds and faults orientated approximately N-S, NE-SW, NW-SE, and E-W (Figures 2 and 4). Despite the superimposed contractional deformation, it is possible to distinguish the fold and fault geometries typical of extensional settings, most notably listric normal faults and rollover anticlines.

[16] The best-developed structure is the Sapagua half graben (SHG) with an infill of growth strata that thicken into the bounding listric fault. The Ovara half graben (OHG) to the south is narrower and less pronounced. Both half grabens are overlain by a postrift succession that is virtually undeformed except for westward tilting. This suggests that the two half grabens have not undergone any substantial inversion. Several curved faults trending NW-SE to W-E delimit the Sapagua and Ovara half grabens, within which they are contained. The configuration of these faults and their associated folds are described in the following sections. The faults are labeled F1–F5 in Figures 4 and 5.

3.3.1. Sapagua Half Graben

[17] The Sapagua half graben is limited to the north by fault F5 (Figure 4), which has a vertical throw of approximately 1500 m and a large associated rollover fold in its hanging wall. The fault vanishes in the upper part of the synrift deposits. Its plane has been rotated between approximately 50 and 80° to the west on the steeply inclined west flank of a major Neogene anticline. This rotation and subsequent erosion have exposed its listric geometry at depth. The original strike of the fault plane was approximately E-W, parallel to the axis of the monocline developed in the postrift deposits sealing the fault. A direct means of determining the geometry of the half graben is to view the geologic map in down plunge direction [*Mackin*, 1950], looking at Figures 4 and 5 from the east. This provides an excellent cross-section view of the half graben and the accompanying anticline in the Pirgua subgroup synrift deposits.

[18] Even though the outcrops are partly covered by a thin veneer of scree, the geometry of the strata that compose the rollover can be easily traced on aerial photographs and satellite images (Figures 4 and 5). The synrift deposits in the hanging wall of fault F5 comprise deposits of eolian and fluvial origin and of nonchannelized debris flows, arranged in the order shown in Figure 5. The strata show a markedly

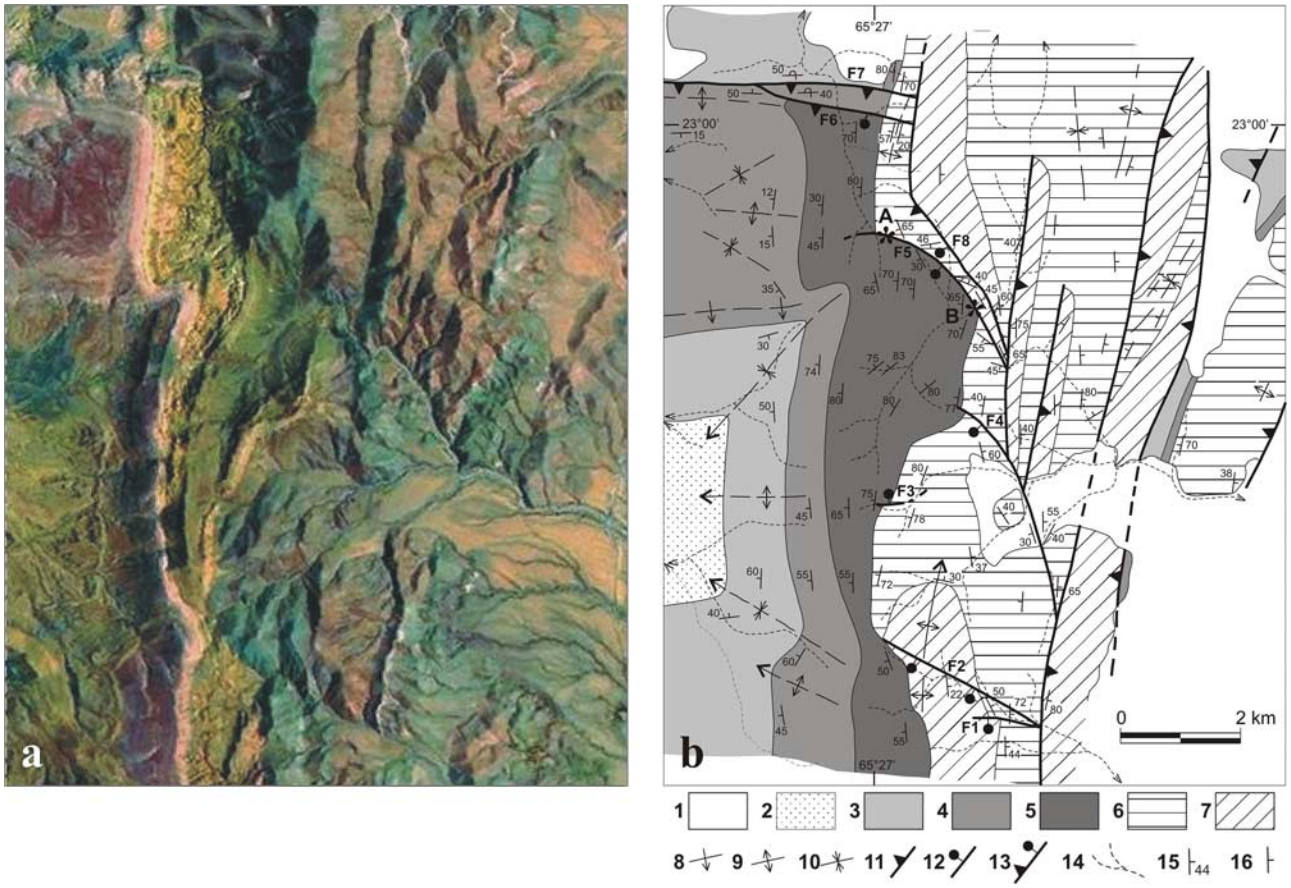

Figure 4. (a) Part of Landsat thematic mapper (TM) scene comprising the Sapagua area. (b) Structural interpretation: 1, Quaternary; 2, Tertiary; 3, Santa Bárbara subgroup; 4, Balbuena subgroup; 5, Pirgua subgroup; 6, Ordovician; 7, Cambrian; 8, monocline; 9, anticline; 10, syncline; 11, thrust or reverse fault; 12, normal fault; 13, reactivated normal fault; 14, stream; 15, strike and dip measured in the field; 16, strike and dip interpreted from aerial photo. A and B are localities where fault F5 is exposed.

diverging geometry and thicken progressively to a maximum of approximately 1800 m near the fault plane (Figure 6a). With increasing distance from the fault the synrift succession thins to a minimum of no more than 200 m over the hinge of the hanging wall. A marked thinning of the Ordovician prerift succession due to erosion can be observed in the same direction.

[19] Only the upper eolian sequence was deposited on the footwall of normal fault F5, the main fault of the half graben, with a thickness of approximately 400 m. Farther north, the synrift deposits terminate against the footwall of fault F6.

[20] The fluvial and debris flow deposits involved in the rollover show internal onlap and offlap relations, indicating processes of prograding and retrograding deposition. We interpret these to reflect variations in the ratio of depositional rate to the rate of subsidence or creation of accommodation space, directly related to the velocity of displacement of fault F5. Climatic variations may also have been influential. The onlapping and offlapping stratal geometries, combined with progressive downward tilting caused by the incremental displacement on fault F5, have created erosional and partly angular unconformities in the synrift growth strata that form the rollover. This does not necessarily indicate different deformation events since the thickest section of the half-graben fill, close to the fault plane, is entirely conformable (Figure 5). Fault F5 is exposed in two localities (A and B in Figure 4). Despite its throw of about 1500 m, the damage zone of the fault is no wider than 10–20 m. In both localities the hanging wall strata consist of Pirgua subgroup sedimentary breccias. In locality A (Figure 6b) the fault core comprises approximately 2 cm of clay gouge and up to 0.6 m of cohesionless, finely brecciated gouge material originated from Ordovician siltstones and sandstones. The footwall consists of Ordovician quartzites with finer-grained intercalations. Although the resistant beds are intensely fractured, bedding is easily recognizable and dips steeply southwest into the fault. Secondary faults offsetting the quartzite beds appear as very steep reverse faults, but may constitute rotated normal faults (Figure 6c). In locality B the fault core consists of pelitic to fine sandy material, exhibiting a steeply dipping, southeast-striking, parallel-to-lenticular fabric with finely striated fragments. Thin striated calcite veins at a few centimetres

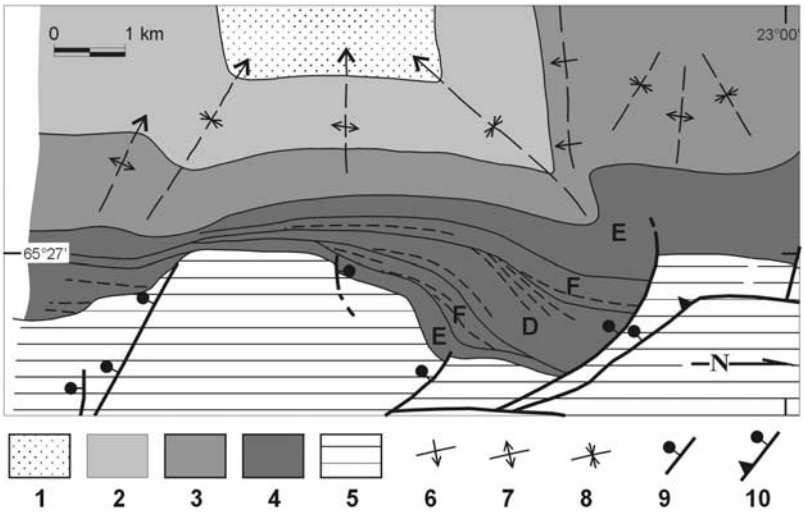

Figure 5. Map of the synrift sequences in the Sapagua half graben, with different facies shown. Notice traces of beds (dashed lines) diverging into the main bounding fault. The map is shown with north to the right to enable a westward, down plunge view of the structures (see text), particularly the half graben and the rollover anticline. Facies symbols: E, eolian; F, fluvial; D, debris flow sequences. 1, Tertiary; 2, Santa Bárbara subgroup, 3, Balbuena subgroup; 4, Pirgua subgroup; 5, Cambrian and Ordovician; 6, monocline; 7, anticline; 8, syncline; 9, normal fault; 10, reactivated normal fault.

spacing parallel this fabric or dip moderately steeply into the fault. Less than 1 m of the fault core is exposed. Unfractured Cambrian quartzites of the footwall crop out, dipping eastward, a few tens of meters to the north. A notable structure associated with fault F5 is the monocline situated above its termination within the synrift deposits (Figures 4 and 5). This structure, with E-W trending axis, is very well developed in the postrift deposits (Figure 6a). We attribute it to an extensional fault-propagation fold formed by late normal reactivation of fault F5 during the postrift stage. Differential compaction can also have contributed to the formation of the monoclines, as has been postulated for other extensional basins (e.g., the Sirte basin of Libya [*Skuce*, 1996]).

[21] Toward the south, in the hanging wall of fault F5, there are two other faults (F4 and F3) of less vertical throw but similar listric geometry. Fault F4 is synthetic and fault F3 antithetic with respect to the listric master fault F5. Restoring the rotation caused by Neogene folding shows that both faults originally had an E-W strike parallel to the master fault.

[22] Faults F3 and F4 terminate upward in the basal section of the synrift deposits and exerted some control on its thickness, whereas fault F5 strongly controlled the thickness of the upper synrift sequences (Figure 5). This indicates that they were not activated simultaneously and that the propagation direction for the Sapagua half graben was from south to north toward the footwall.

3.3.2. Ovara Half Graben

[23] The Ovara half graben developed in the hanging wall of faults F2 and F1, which mark its border with the northerly adjacent Sapagua half graben (Figures 2 and 4). Faults F2 and F1 converge downward (eastward), suggesting that both are splays of a single normal fault. Close to the junction of faults F2 and F1 this extensional system is dissected by a west-directed thrust fault, but we could not identify the deeper portions of the normal fault in its footwall. The exposed parts of faults F2 and F1 seem to have planar geometries. Both faults only affect the prerift strata, and a monocline dipping into the half graben is developed above their terminations. The synrift strata progressively onlap the monocline. This geometry suggests extensional fault-propagation folding associated with "trishear" deformation [*Erslev*, 1991; *Allmendinger*, 1998] between the two faults that may have fairly minor displacements. Gentle WNW-ESE trending folds, similar to those in the SHG but less accentuated, are also present in the postrift strata of the OHG. It is evident that the Ovara half graben was activated first, since its synrift deposits are largely overstepped by the basal synrift strata of the SHG, indicating the time when both became connected (Figure 5). During the climax of rifting the extensional faulting was concentrated in the SHG, as evidenced by the thicker strata deposited there. At that time the OHG was practically inactive and subsided passively along with the SHG. This is in keeping with the northward propagation of faulting observed within the SHG.

[24] The relations between the SHG and OHG show that (1) at least locally there is a clear south-to-north propagation of transverse normal faulting in the Tres Cruces rift, and (2) there can be marked differences in the age of the synrift deposits in adjacent structures because of diachronous activation. If this is not taken into account, erroneous correlations may result, particularly for the basal sections.

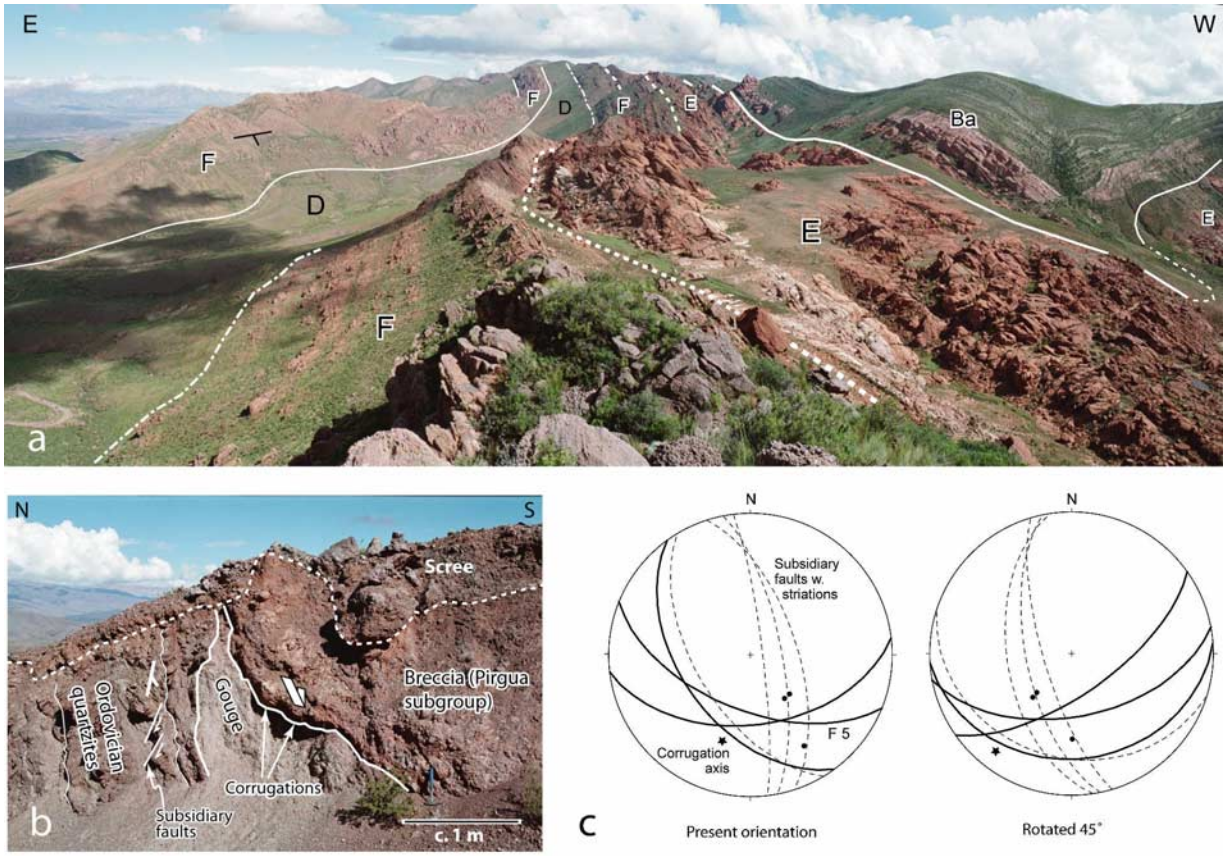

Figure 6. (a) Panoramic view toward the south along the Sapagua half graben. Point of view is just south of the main fault F5 and slightly west of locality A as indicated in Figure 4 and shown in Figure 6b. Compare structure and facies pattern to Figure 5. Facies symbols in Pirgua synrift strata are F, fluvial; D, debris flows; E, eolian. The base of the synrift fill is not visible on this photo. Ba is Balbuena subgroup (basal postrift). On the far right, part of the monocline above the termination of fault F5 can be seen. (b) Fault F5 on outcrop at locality A. Notice corrugations of the main fault plane and subsidiary faults. (c) Stereonet representations of structural features shown in Figure 6b, in present-day orientation (left) and rotated 45° to the east about a horizontal, north-trending axis to restore original configuration (right). Undulating surface of fault F5 is represented by three planes (great circles). Rotated subsidiary faults appear as normal faults. Rotated corrugation axes suggest dextral strike-slip component.

3.3.3. Nature of the E-W-Trending Normal Faults

[25] In extensional tectonic settings the pattern of normal faulting is typically dominated by longitudinal faults that are parallel or subparallel to the basin axis and to a lesser degree by oblique or transverse faults [*Harding*, 1984]. Since the axis of the Tres Cruces subbasin has a well-defined N-S trend (Figure 1), it can be assumed that the principal border fault systems had similar strikes and that the faults and half grabens described in sections 3.3.1 and 3.3.2 are transverse structures. Transverse faults on rift borders have been frequently mentioned and designated with different terms (e.g., transfer fault [*Gibbs*, 1984], transverse fault [*Letouzey*, 1986], and cross fault [*Morley et al.*, 1990]), although the term transfer fault has become most widely used. According to the definition of *Gibbs* [1984], transfer faults link coeval extensional faults of different displacement rates and have an important strike-slip motion component.

[26] *Destro* [1995] recognized another type of transverse fault which he termed release fault. Release faults have geometric characteristics similar to transfer faults but are genetically unrelated. According to *Destro*'s [1995] model, release faults are transverse faults that form to accommodate fault-parallel extension of the hanging wall. Such extension results from bending caused by along-strike displacement variations on a normal fault. The bending stress is released by brittle failure, resulting in the formation of release faults (Figure 7). Release faults are characterized by striking perpendicular or obliquely to the longitudinal normal faults of the rift. They do not necessarily depend on preexisting weak zones. They are localized in individual hanging walls, do not connect different normal faults and show predominantly dip-slip displacement, with maximum slip near the associated longitudinal normal fault.

[27] There is no evidence that the transverse faults associated with the SHG and OHG (F1 to F5) are transfer

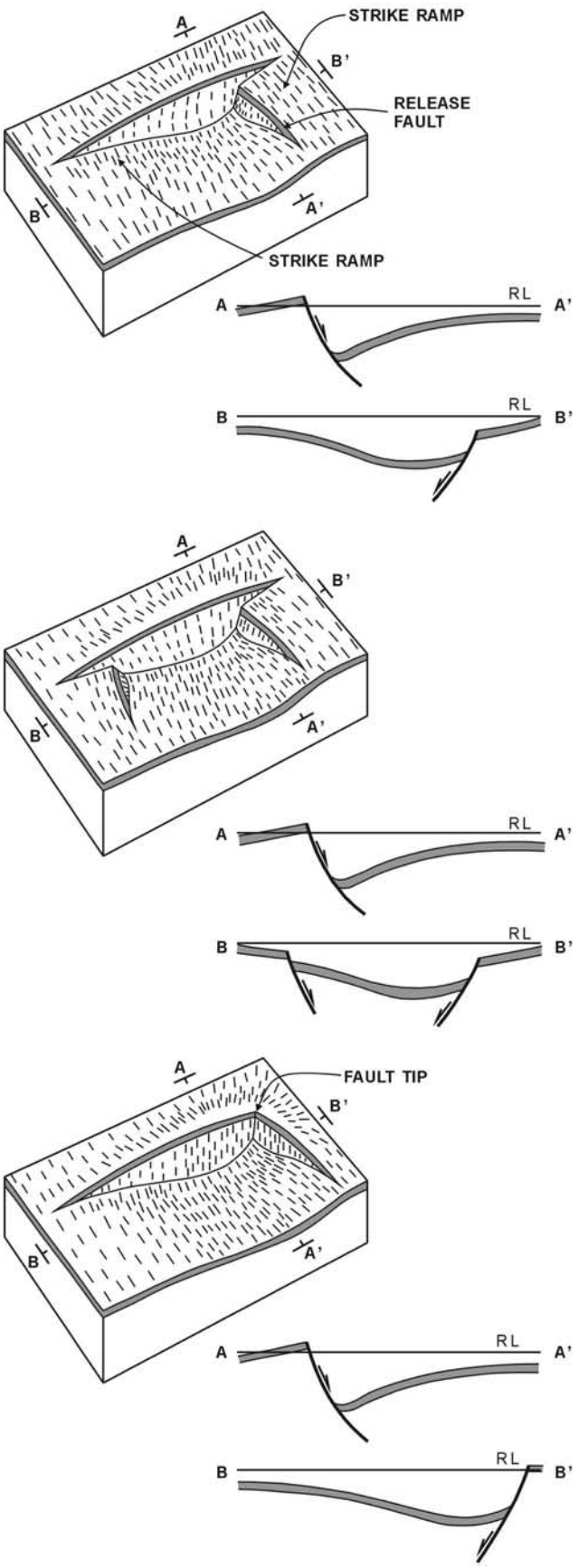

faults in a stepped longitudinal system. We assume they are release faults to a north-striking master fault farther east, now masked by Cenozoic deformation (see, e.g., the Negra Muerta fault described in section 3.4.2).

3.3.4. Geometric Modeling of the Sapagua Half Graben

[28] The anticline of the Sapagua half graben is a typical rollover (or reverse drag [*Hamblin*, 1965]) fold. These folds result from the movement on upward concave listric faults and hence can be regarded as extensional fault-bend folds [*Mitra*, 1993]. The geometric and kinematic evolution of these folds have been discussed by many authors, essentially on the basis of examples imaged in seismic reflection profiles, but also on geometric and analogue models [e.g., *Gibbs*, 1983; *Davison*, 1986; *White et al.*, 1986; *McClay and Ellis*, 1987; *Williams and Vann*, 1987; *Dula*, 1991; *Xiao and Suppe*, 1992; *Withjack et al.*, 1995; *Hauge and Gray*, 1996; *Shaw et al.*, 1997].

[29] In order to compare fault F5 and the Sapagua half graben to idealized models of extensional structures we used simple geometric modeling to extrapolate the fault geometry beyond the exposed trace and to analyze the evolution of the half-graben fill. We converted the map view of the half graben (Figure 4) to a true cross section by correcting for the somewhat different regional dips along the structure. This resulted in only slight geometric adjustments. We did not include the relatively tight fold above the fault tip in the uppermost synrift and overlying postrift strata. Although this fold probably originated as an extensional fault-propagation fold (see 3.3.1), associated thrust faults indicate that it tightened later during mild inversion that did not affect the deeper parts of the half graben (Figure 6a). We therefore assumed in the models a gentle monocline to connect the top of synrift strata in the hanging wall and footwall.

[30] Probably the most commonly applied geometric model for extensional settings is hanging wall deformation by inclined shear, often with the shearing planes dipping at the same angle as the master normal fault but antithetically to it. This allows the geometry of the fault at depth to be constructed from the shape of the hanging wall [*Dula*, 1991]. Attempts to model the fault shape from the total displacement of the top basement surface in a single step gave no satisfactory result because of a strong misfit between hanging wall and footwall cutoff angles as constrained by mapping (Figures 4 and 5). A stepwise qualitative restoration (Figure 8) suggested that the low hanging-wall cutoff angle observed near the visible base of fault F5 may correspond to a part of the footwall that was eroded during the evolution of the half graben and that the conspicuous hanging wall syncline filled in by fluvial facies (Figures 5 and 6a) was caused by fault-bend folding above a low-angle segment of fault F5. On the basis of this assumption we calculated fault geometries from hanging wall shapes for each consecutive step, using Midland

Figure 7. Characteristics of release faults caused by displacement variations on a master fault. (Modified from *Destro* [1995] with permission from Elsevier.) RL is regional level. Compare lowermost block diagram with Figure 12.

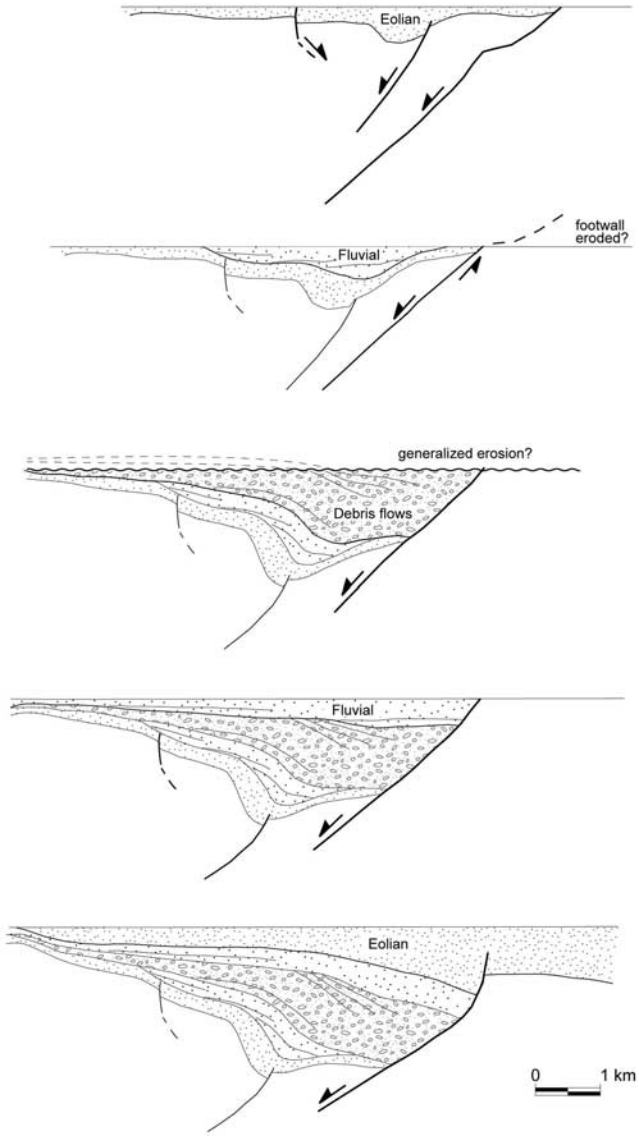

Figure 8. Evolution of the Sapagua half-graben fill, produced through qualitative stepwise restoration of the map in Figure 5.

Valley's 2DMove software. The calculated detachment depths increase from just above 2 km to almost 4 km depth below a reference point in the footwall from step 1 to step 4 (Figure 9a). We consider it unlikely that the master fault has actually cut progressively into its footwall, thus adding material to the hanging wall. Alternatively, the assumption of a fixed footwall may not strictly hold, and the half-graben subsidence could reflect a combination of fault-controlled subsidence with a synclinal depression of the footwall as shown in Figure 9b. Nevertheless, the strong widening of the half graben in step 4 suggests that the basal detachment at just about 2 km depth was ultimately abandoned in favor of a deeper one at almost 4 km depth. Even though the depth to the detachment(s) is not well constrained, it is clear that the north-trending fault which today delimits the Sapagua half graben to the east (Figure 4) is not the exposed basal detachment of fault F5 but a younger thrust fault which truncates the extensional structures. Flattening of the listric fault at depths of 2–4 km corresponds to detachment levels in the Puncoviscana formation. This is consistent with the décollement levels observed for many Neogene thrust faults of the Eastern Cordillera. The total amount of horizontal extension on normal fault F5 is approximately 2 km.

3.4. Structures Indicating Fault Reactivation

3.4.1. Faults Trending East

[31] The northernmost part of the SHG is delimited by two E-W-trending, south-dipping, interconnected faults F6 and F7 (Figures 2 and 4). The Pirgua subgroup synrift deposits terminate against fault F6. Immediately to the north, the postrift strata of the Balbuena subgroup directly overlie Paleozoic rocks, demonstrating the normal fault origin of F6. This fault was inverted during the Neogene contractional deformation and initially generated a fault-propagation fold in the postrift strata, which was then dissected as the fault propagated toward the surface. Simultaneously or later, a minor short cut (fault F7) developed in the footwall of fault F6. The fault-propagation fold created by the inversion of fault F6 has an E-W trending axis, a short and steeply inclined forelimb, and a long gently dipping backlimb. Toward the west the fold axis is strongly curved and swings into a N-S trend, more compatible with the Neogene shortening direction (Figure 2). Although their orientation would suggest that faults F6 and F7 should have important strike-slip components, the striations observed in their vicinity all indicate dip-slip reverse motion. We only found a few slickensides indicative of dextral strike-slip motion at one location immediately north of fault F7. These planes dissect others with kinematic indicators of pure reverse motion. Curved fold axes in the Esquinas Blancas structure, north of fault F7, also indicate dextral horizontal displacement. These observations suggest that the strike-slip motions on faults F6 and F7 occurred in a late phase of the Neogene deformation and that they were of smaller magnitude than the dip-slip motion.

3.4.2. Faults Trending North

[32] The Vicuñayoc-Barro Negro and Negra Muerta thrusts (Figure 2), both verging to the east and 40–50 km long, are important N-S-trending faults with evidence for inversion in the area investigated. Seismic lines suggest fanning reflectors and increasing thickness of the synrift deposits into the Vicuñayoc-Barro Negro fault and reverse displacement of reflectors corresponding to the postrift strata [*Kley et al.*, 2005]. Farther north, near the village of Tres Cruces, the fault displacement decreases and a null point appears to be exposed at the surface (Figure 2).

[33] The Negra Muerta fault may be an important reactivated border fault of the rift, because in its footwall only a strongly reduced thickness of postrift strata is present, and the lower parts are missing entirely (Lecho formation and lower member of the Yacoraite formation). However, as in many comparable cases, it cannot be demonstrated that the

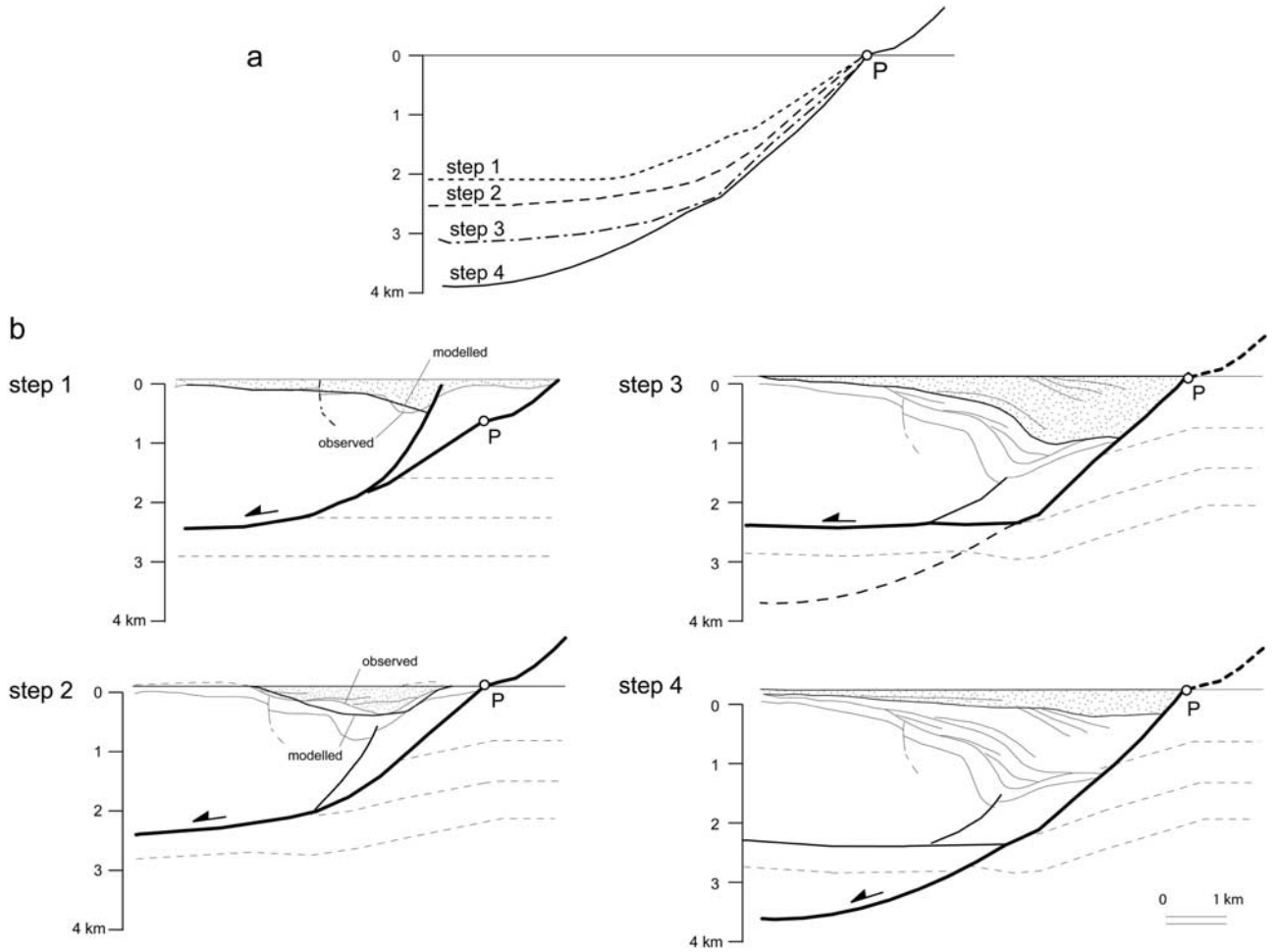

Figure 9. Stepwise geometric modeling of fault geometry from the shape of the hanging wall in the Sapagua half graben using vertical shear to simulate hanging wall deformation. (a) Changing half-graben geometries through time suggest increasing detachment depth. (b) Gentle footwall deformation allows the same fault to remain active in steps 1–3. A deeper detachment only originates in step 4. Strata deposited during each step are patterned.

thrust fault separating rift-basin and rift-shoulder sequences is actually the reactivated normal fault, because synrift deposits on the hanging wall side are only preserved several kilometers away from the fault. At any rate, normal displacement here seems to have persisted into the sagging stage, controlling the deposition of the basal postrift strata. However, residual rift relief may also account for the thinned postrift strata.

[34] Between the structures of Sapagua-Ovara-Queñoal and the Negra Muerta fault there is a predominantly north-trending swath of faulting and brecciation. Fault vergences are both toward the east and west (backthrusts). In this area the synrift deposits apparently have been completely eroded. Even though the majority of the faults appear to have reverse displacements, it is probable that some of them are inherited rift faults rotated during Neogene deformation.

[35] In the far north of the Sapagua half graben the transverse faults F5–F7 are connected to fault F8 of curved trace, N-S strike, and westward dip (Figure 4). The stratigraphic relationships along fault F8 indicate normal displacement in the north and reverse displacement in the south, suggesting that it is a Cretaceous normal fault that transferred displacement from fault F5 in the south to fault F6 in the north and was later reactivated by Neogene compression.

3.4.3. Anticlines at Fault Intersections

[36] A conspicuous feature observable on geologic maps, aerial photos, and satellite images (Figures 2, 10, and 11) is the spur-shaped termination or closure of some broad, dome-shaped anticlines. The spurs are outlined very clearly by the limestone marker beds of the Yacoraite formation (Balbuena subgroup). The most representative examples are the gently plunging southward extensions of the Esquinas Blancas, Cerro Queñoal, and Cerro Colorado anticlines. A similar structure is insinuated in the southernmost part of the SHG (Figure 4), but no complete anticline in the

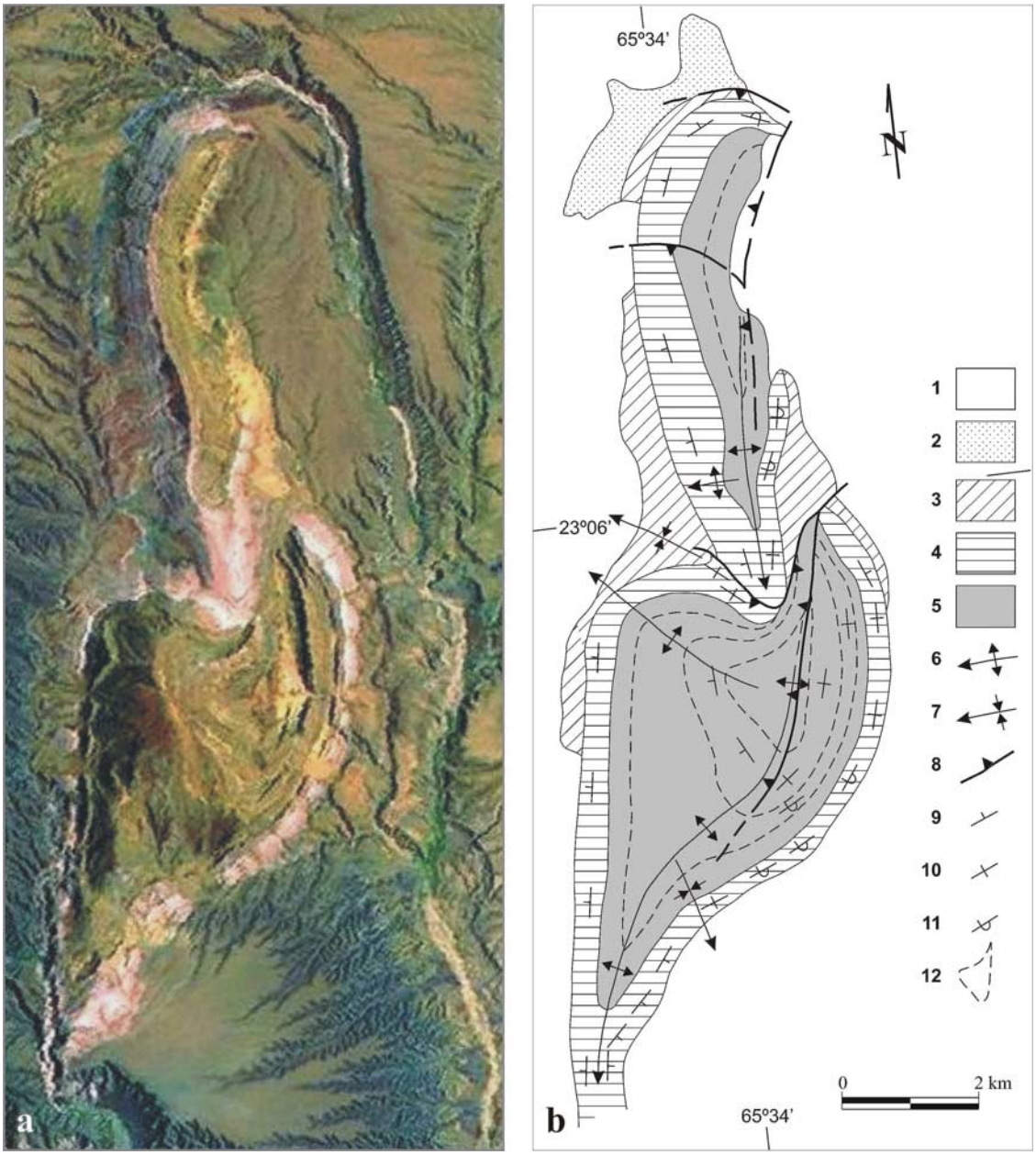

Figure 10. (a) Part of a Landsat TM scene showing Cerro Colorado. (b) Structural interpretation. 1, Quaternary; 2, Tertiary; 3, Santa Bárbara subgroup; 4, Balbuena subgroup; 5, Pirgua subgroup; 6, anticline; 7, syncline; 8, reverse fault; 9–11, strike and dip of bedding (9, 30–60°; 10, 80–90°; 11, overturned); 12, form line of bedding.

Yacoraite formation is present here. Nevertheless, the coincidence of this spur with the southward thinning synrift deposits is the most direct evidence that these peculiar features reflect thickness variations of the Pirgua subgroup; although the next exposed Pirgua successions south of Cerro Queñoal and Cerro Colorado are also markedly thinner than those in the cores of the two anticlines.

[37] A qualitative model to explain the dome-shaped anticlines with spur-like terminations is shown in the block diagram of Figure 12. It is based on the observations above and on the fact that the Cerro Queñoal and Cerro Colorado anticlines are both associated with north- and east-trending thrust or reverse faults. The model assumes a half graben formed by the interaction of a longitudinal normal fault with a transverse (release?) fault, both of listric geometry and with lateral terminations. If the half graben is completely filled by synrift deposits, the infill forms an approximately tetrahedrical body with four triangular faces: (1) the plane of the longitudinal normal fault, (2) the plane of the transverse release fault, (3) the base of the synrift strata, and (4) the top

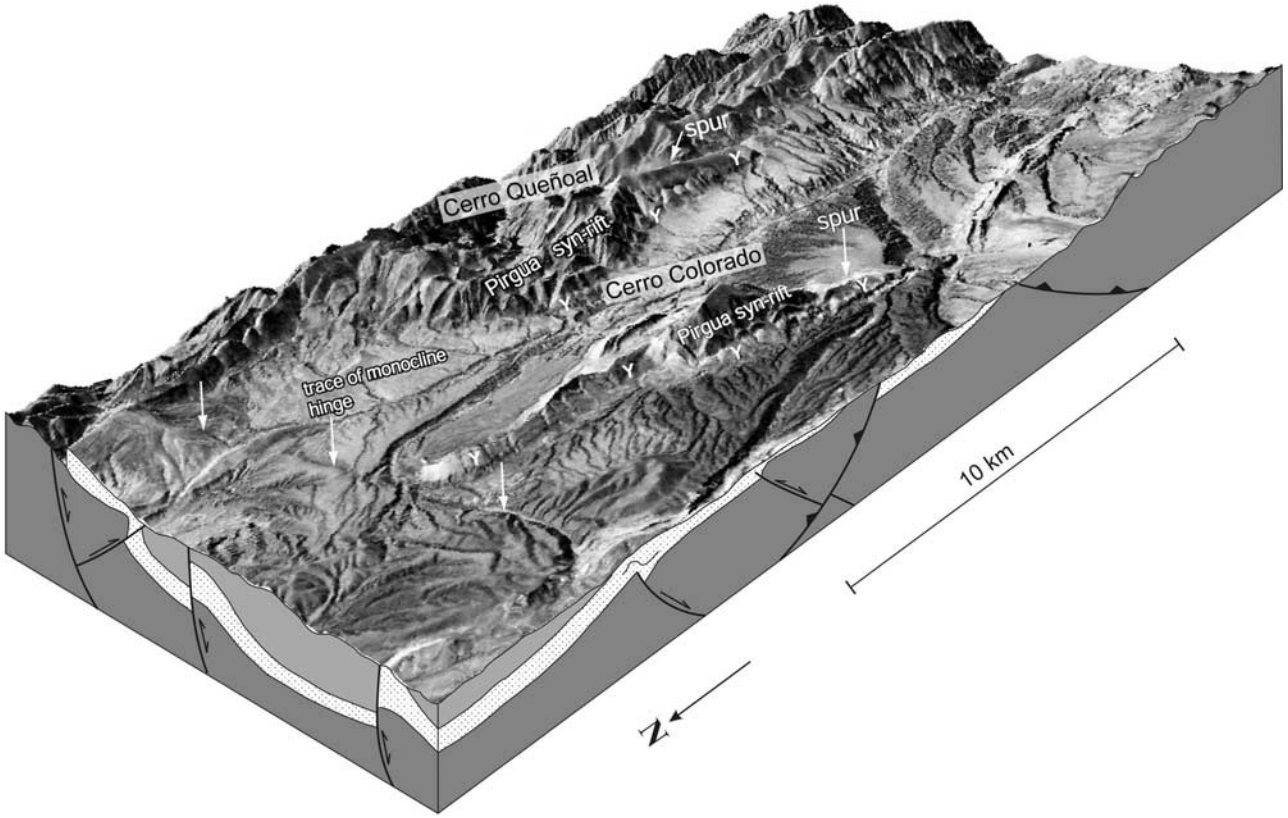

Figure 11. Synthetic oblique view of Cerro Colorado and Cerro Queñoal, created by overlaying part of a Landsat TM7 scene on the NASA Shuttle Radar Topographic Mission 90 digital elevation model (compare to Figures 2 and 10). Note broad central anticlines with exposed synrift strata and spur-shaped extensions in the postrift succession. Yacoraite marker horizon (indicated by Y) appears whitish. Normal longitudinal and transverse faults, both preserved (single-headed arrow) and reactivated (double-headed arrow), are schematically shown in the two orthogonal structural sections of the block diagram.

of the synrift strata. Of the six tetrahedron edges, four are hanging wall cutoff lines of the base and top, respectively, of the synrift deposits on both faults; one is the fault intersection line, and one is the hanging wall hinge line which ideally also corresponds to the pinch out of the synrift strata in the hanging wall.

[38] As this configuration undergoes contraction, the inversion of the half graben and reactivation of the faults provokes the deformation of the overlapping postrift cover by a process of fault-propagation folding [*Suppe and Medwedeff*, 1990] or forced folding [*Stearns*, 1978]. Fault propagation will originate folds with short, steep to overturned forelimbs and longer gently inclined backlimbs in the postrift strata. At the same time the inversion of the tetrahedrical wedge of synrift deposits will lift up the postrift cover and form an anticlinal culmination coinciding with the greatest thickness of synrift deposits near the intersection of the two faults and with gentle plunges toward the areas of minimum thickness. A buttressing effect of the faults may cause tight folding of the prerift and synrift strata.

[39] The simple deformation history suggested by this model could be complicated by the generation of new faults during inversion and by more complex geometries of the inverted faults. For example, the abrupt decrease of fold wavelength at the transitions to the spurs indicates a sudden shallowing of the detachment level that is not included in the model. Even so, the southern part of the Cerro Colorado anticline (Figure 10), dome shaped and approximately triangular in map view, coincides reasonably well with the model in the following aspects: (1) It is limited to the north by a transverse fault and dissected in the east by a longitudinal fault, both curved and possibly inverted; (2) its north and east limbs are very steep and in part overturned, while the western (back) limb dips more gently; (3) the anticlinal culmination is located in the northeast corner, close to the fault intersection; (4) the anticline has spur-shaped terminations plunging toward the northwest and south; and (5) its exposed core in synrift strata is tightly folded. We attribute the markedly curved trace of the transverse fault to folding during the inversion process, particularly near its intersection with the longitudinal fault where deformation may have concentrated. A striking feature of the Cerro Colorado structure is the abrupt change in folding style across the transverse fault, suggesting that

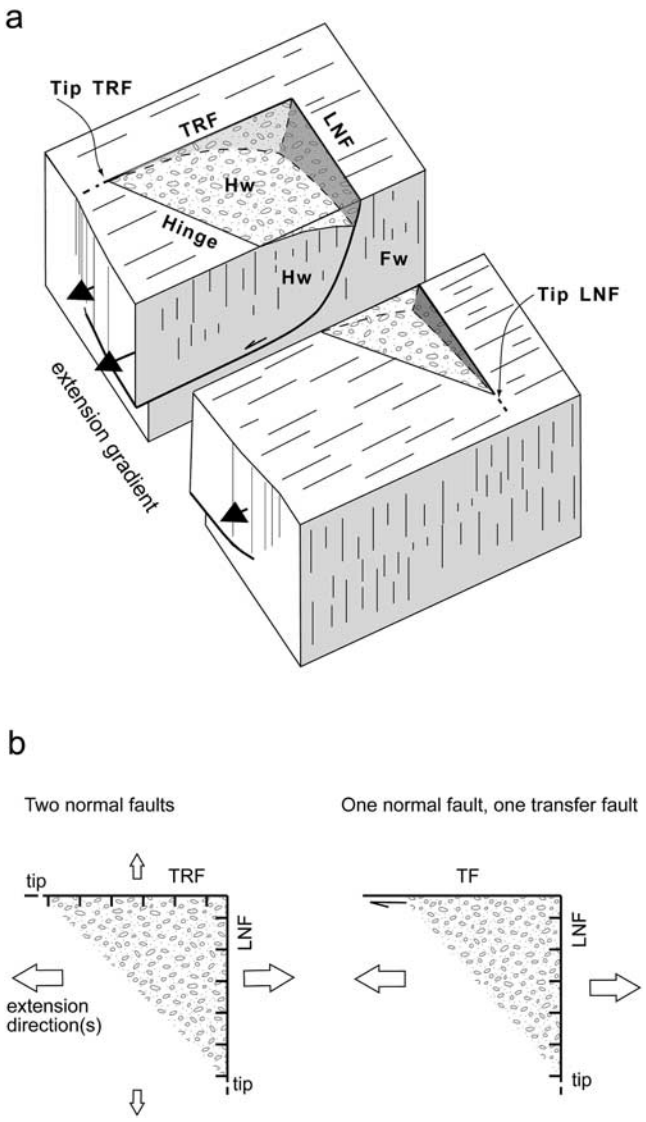

Figure 12. (a) Schematic block diagram showing the tetrahedron-shaped body of synrift deposits produced near the intersection of a longitudinal normal fault (LNF) and a transverse release fault (TRF). Hw, hanging wall; Fw, footwall. (b) Similar synrift geometries result regardless of if the transverse fault is a transfer fault or release fault.

the latter has induced compartmentalized deformation [*Wang et al.*, 1995].

[40] The Cerro Queñoal structure is an approximate, if larger, mirror image of the southern part of Cerro Colorado (Figures 2 and 11), with a steep to overturned west limb. It is more complex and less complete because it is dissected by a N-S striking, probably Neogene longitudinal fault, exhibits internal folding and is truncated in the east by a thrust fault. Despite these complications, both folds appear to have similar controls. The Cerro Queñoal anticlinorium terminates in the north against an important transverse reverse fault. The approximately 9 km long fault trace is curved, changing from a NW-SE to an E-W trend (Figure 2), and the fault plane dips south to southwest. Toward the west the transverse fault appears to connect with or to intersect another curved reverse fault that trends NW-SE to N-S and dips to the east. This fault cuts the steep to overturned strata in the west limb of the anticlinorium, suggesting that it may also have originated as a normal fault and that reverse propagation during the first stages of inversion has produced the steeply dipping western fold limb. In the east the main fault has a splay that also trends N-S but dips to the west. There are no clear indications as to the kinematics of this west-dipping fault, making it difficult to establish if it formed as an antithetic Cretaceous normal fault or as a Neogene backthrust linked to and coeval with the inversion of the main fault in the west. The transverse Queñoal reverse fault connects the tips of N-S trending faults of opposite dip and has a dextral strike-slip component, as indicated by the curved fold axes of the anticlinorium. It has therefore acted as a transfer fault during inversion but may have originated as a rift transfer fault.

4. Discussion

[41] The observations on outcrops in the Tres Cruces rift segment analyzed in this paper provide some first guidelines for the interpretation of structures in the Salta rift. Gentle folding or monoclines in the postrift sequence above normal fault tips have been observed on seismic lines from the Olmedo subbasin and were attributed to inversion and transpressive strike-slip motion (Figure 13) [*Chiarenza and Ponzoni*, 1989; *Comínguez and Ramos*, 1995; *Bianucci*, 1999]. However, the similarity with the structures above the SHG and OHG suggests they could rather be due to minor normal reactivation with extensional fault-propagation folding that occurred during the ''sagging'' or thermal subsidence stage and possibly to added effects of differential compaction that created drape folds in the post-rift strata. A late and very subdued extensional tectonic phase, which presumably occurred during the sagging stage recorded by the Balbuena and Santa Bárbara subgroups, has been recognized on seismic lines from other parts of the basin and was termed ''pre-Olmedo tectonics'' (H. A. Bianucci et al., unpublished report, 1980). These episodes are coeval with basalts known from outcrops in the Sierra de Zapla (Las Capillas and Corral de Piedras rivers) and from several petroleum exploration wells (Fraile Pintado, Caimancito, and Las Colmenas (A. Boll et al., unpublished report, 1989)). They may also have played a role in the creation of the lacustrine basin of the Maíz Gordo formation (Lower Eocene).

[42] In the Olmedo example (Figure 13) our interpretation is corroborated by the fact that the monoclines only affect the postrift strata and are strongly attenuated or vanish in the overlying synorogenic foreland deposits. A correct interpretation of such structures is crucial for defining the age of initial Andean shortening [cf., *Hongn et al.*, 2007].

[43] Unconformable relationships observed in seismic lines from the Salta rift (Figure 14) were often interpreted as the base of the synrift strata [*Bianucci et al.*, 1982;

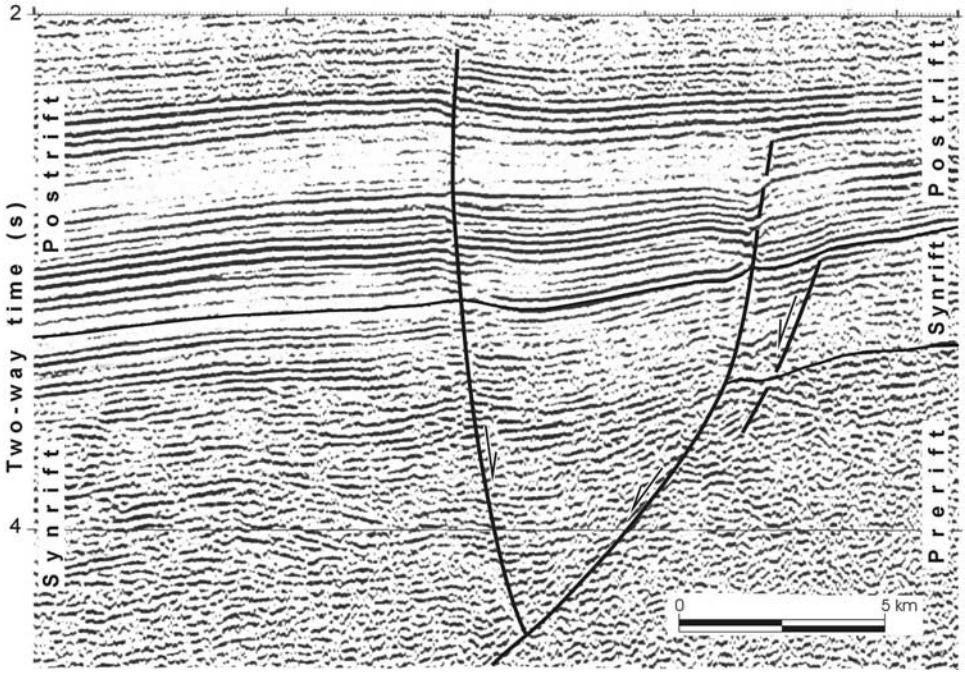

Figure 13. Seismic line from the Lomas de Olmedo subbasin, exaggerated vertically approximately four times. (Reinterpreted from *Comínguez and Ramos* [1995].) We interpret the minor folds in the postrift sequence as fault-propagation folds produced by late extensional reactivation of some rift faults in Eocene (?) time.

Uliana et al., 1995], although some of these discontinuities might well be unconformities within the synrift succession as present in the SHG (see contrasting interpretations of the same regional seismic line by *Comínguez and Ramos* [1995] and *Starck* [1995]). The surfaces that truncate reflectors and the onlapping geometries of the overlying strata need to be carefully analyzed in order to correctly identify their stratigraphic positions. The location of the hinge line controlling the rotation of the hanging wall should closely reflect the fault geometry and remain more or less fixed with respect to the footwall during progressive extension. Consequently, the first (prerift to synrift) unconformity formed over the hinge will migrate away from the footwall while a new hinge and possibly a new unconformity will form in the growth strata. Ideally, this will result in a series of fanning unconformities of which the oldest is most distant from the footwall (Figure 14).

[44] In a more general way the data now available from the Salta rift provide constraints on the conditions for fault reactivation. It has long been recognized that the reverse reactivation of normal faults presents a mechanical problem. At the typical friction coefficients measured in laboratory experiments, new ideally oriented thrust faults will nucleate before the relatively low resolved shear stress on steeply dipping faults reaches the critical value for frictional sliding [e.g., *Sibson*, 1995]. Beyond a certain dip value that depends on the friction coefficient the shear stress on the fault plane will never overcome the normal stress and ''frictional lockup'' prevents any fault reactivation. Analogue models of inversion using sand or comparable materials and not enforcing particular fault geometries indeed show that few extensional faults become reactivated, and that graben inversion is mostly achieved by newly formed thrust faults (see *Panien et al.* [2005] for a review). *Brun and Nalpas* [1996] showed that steep normal faults can reactivate as transpressive strike-slip faults if the rift is shortened at a low angle to its axis. This led them to conclude that normal fault reactivation was in general the result of oblique inversion. In contrast, many studies of natural examples suggest that fault reactivation occurred under nearly orthogonal contraction. One solution to this paradox is elevated fluid pressure that can induce ''fault valving'' and reverse motion on steeply dipping faults [*Sibson*, 1995, 2004]. Another solution is low mechanical strength of the inherited faults [*Buiter and Pfiffner*, 2003]. Strong fluid overpressure is an unlikely cause for fault weakness in the Salta rift. To our knowledge, there is no field evidence such as large veins or hydrofractured and recemented breccias that would indicate a major role of fluids during fault formation or reactivation for any fault in the rift. Also, the prevailing substrate of rocks in low grade metamorphic or very advanced diagenetic state implies that at the burial depths where fault reactivation initiated the only important source of fluids could have been the predominantly sandy or coarser synrift successions.

[45] Those normal faults we have studied in detail have only thin (<1 m) layers of clayey fault gouge and noncohesive pervasively fractured material in their cores (see section 3.3.1). Although these layers are likely to have quite low friction coefficients [*Morrow et al.*, 1982], their reduced

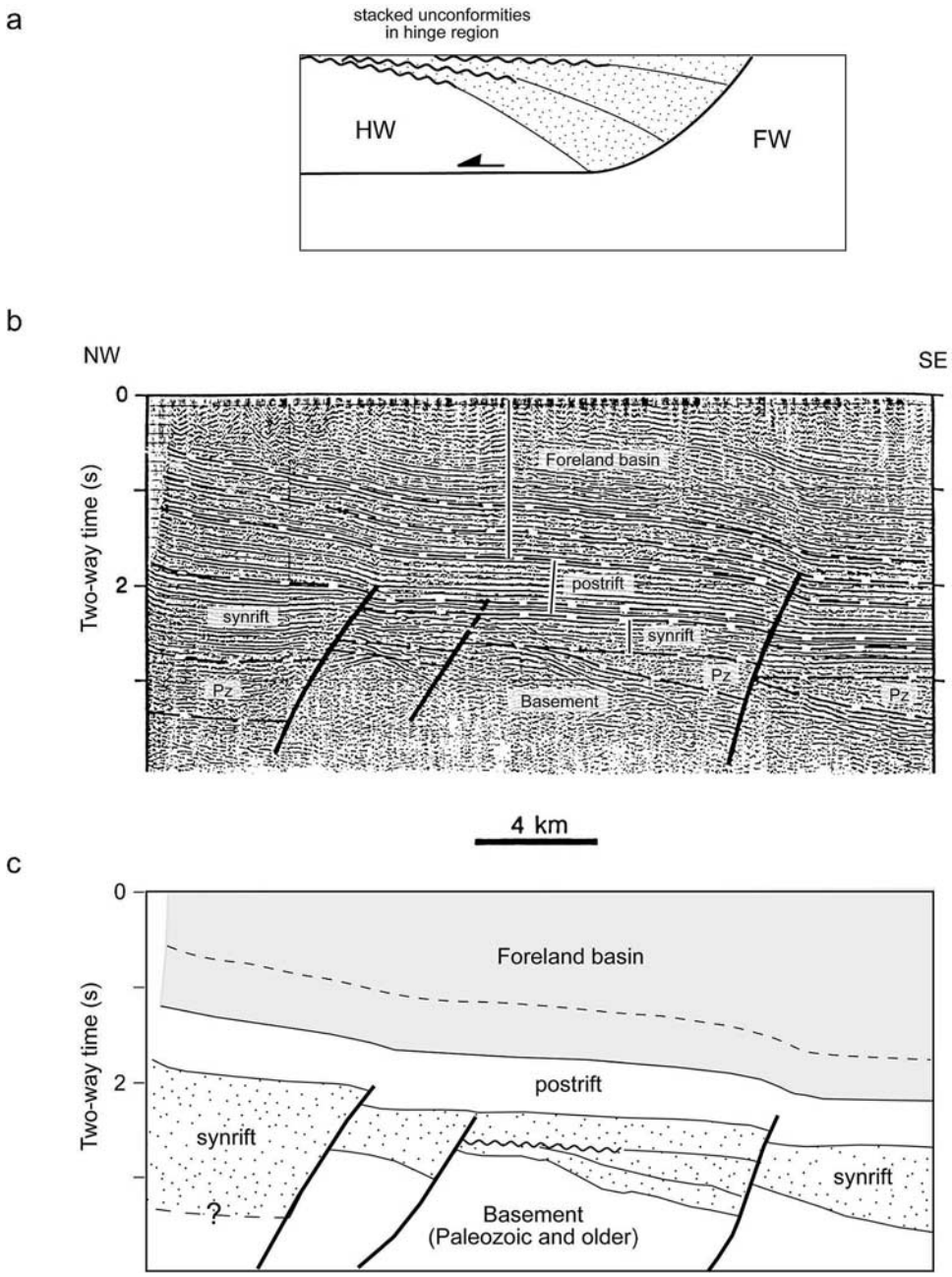

Figure 14. (a) Conceptual model of fanning unconformities in half-graben fill. Deposition just keeps pace with subsidence. Oscillations between deposition and erosion may be induced by varying fault activity or slight fluctuations in base level. (b) Interpreted seismic line of inversion structures in the Lomas de Olmedo subbasin (modified from *Uliana et al.* [1995]). Approximately four times vertically exaggerated. (c) Line drawing of alternative interpretation where the base of coherent reflections is taken to indicate the base of the synrift fill in half grabens similar in size and geometry to the Sapagua structure.

thickness implies that the weakening effect could be counteracted by fairly minor bends of the fault plane with amplitudes of a few meters. In comparison, the numerical models of *Buiter and Pfiffner* [2003] demonstrating the reactivation of weak faults used 600 m thick zones of mechanical weakness for technical reasons.

[46] The inverted Salta rift is well suited to investigate the role of fault orientation because of its good exposure and the relatively simple tectonic setting of the Andes. It is clear that the main, if not only, phase of contraction was more or less perpendicular to the rift, so that overall transpressive inversion can be ruled out. On the other hand, the

Table 1. Properties of Preserved and Reactivated Faults of the Salta Rift[a]

Fault/Locality Name[b]	Dip Azimuth	Angle Between Strike and Contraction Direction	Maximum Original Dip	Geometry	Normal Throw, m	Reactivated	Sources
1 Sapagua (fault F5)	180[c]	0	>50[c]	strongly listric	1500	no	this paper
2 Huacalera	~0[d]	0	~60?[d]	gently listric	<2500	no (strike-slip?)	*Kley et al.* [2005]
3 Purmamarca	270	90	<75	planar?	>1000	moderate reverse (footwall shortcut?)	own unpublished field data, 2007
4 La Yesera	90–120	90–60	~75[e]	strongly listric?	4000?[e]	no, footwall shortcut	*Carrera et al.* [2006]
5 Ayuso	275	85	>60[e]	strongly listric	3000[e]	no, folded	*Carrera et al.* [2006]
6 Cerro Colorado North	280	80	~65[f]	strongly listric	1500[f]	minor reverse, overstepped by low-angle thrust faults	*Kley et al.* [2005]
7 Vicuñayoc	095	85	~50[f]	gently listric	>1500?[f]	reverse	*Kley et al.* [2005]
8 Hornocal	145	35	>70?	gently listric	>4000	dextral transpression	*Amengual and Zanettini* [1973], *Kley et al.* [2005]
9 Cachipunco	120	60	~45[g]	gently listric	500	reverse, slightly dextral	*Kley and Monaldi* [2002]
10 Molinos	060	30	~55[e]	gently listric	5500?[e]	moderate reverse, footwall shortcut	*Carrera et al.* [2006]
11 El Zorrito	350–0	0–10	~45–50?[h]	?	4000?[i]	reverse	*Grier et al.* [1991], *Strecker and Marrett* [1999], and *Carrera et al.* [2006]

[a]The faults are roughly ordered from no reactivation (top) to strong reactivation (bottom).
[b]Their locations are shown in Figure 1.
[c]Corrected for rotation.
[d]Estimated from geologic map.
[e]Measured from cross section interpretation.
[f]Estimated from reflection seismic lines.
[g]Measured from restored cross section.
[h]Present-day dip.
[i]Estimated from kinematic link with La Yesera fault.

normal or transverse rift faults have quite different orientations. Table 1 gives an overview of most of the preserved or reactivated normal faults for which some geometric and kinematic data have been measured or can be estimated. Although the number of faults is limited and the data are often only estimates, the following characteristics seem to emerge:

[47] 1. Those faults virtually unaffected by Cenozoic contraction, including refolding of the fault plane, footwall shortcuts, truncation and the like, and strike E-W, approximately parallel to the Cenozoic contraction direction. A glaring exception is the El Zorrito fault with kinematic evidence for N-S dip-slip reactivation. Minor examples with similar kinematics are faults F6 and F7 described in section 3.4.1.

[48] 2. Reverse reactivation occurs under a wide range of fault orientations (strikes) with respect to the main E-W contraction direction, from about 90 to 30°. The available fault kinematic data are still insufficient to tell if strike-slip components increase with obliquity, although the Hornocal and Cachipunco examples suggest this may be the case.

[49] 3. Many reactivated faults have relatively low dips between 45 and 55°. From about 60–65° dip the likelihood of new footwall shortcut or overstepping thrust faults apparently increases.

[50] 4. Gently listric faults, i.e., those with deeper detachments and larger radii of downdip fault curvature, are preferentially reactivated.

[51] In summary, these data suggest that three factors have favored the reverse to transpressive reactivation of normal faults in the Salta rift: a dip angle lower than approximately 60°, a strike no closer to the contraction direction than approximately 30°, and a low downdip fault curvature. The first two factors indicate that the mechanical strength of the faults and the resolved shear stress on the fault planes are critical and are not independent. As the contraction direction changes from 90 to 0° with respect to the fault strike, an existing normal fault changes from an unfavorably steep potential thrust fault (where a relatively low fault dip may be crucial) over an inclined strike-slip fault (where a low fault dip may be detrimental) to an increasingly unfavorably oriented strike-slip fault. The last factor (fault curvature) suggests that the work required to bend the hanging wall as it moves over the listric fault plays a role or that deep detachments were weaker than shallower ones.

[52] The only structures that do not fit in are those indicative of N-S contraction, which are relatively scarce. There is no consensus as to their significance. One group of authors has suggested they belong to a different, noncoaxial deformation event [*Marrett et al.*, 1994; *Marrett and Strecker*, 2000]. Another group has claimed they were formed by E-W contraction but reflected some kind of interference with inherited (rift) structures [*Mon et al.*, 2004; *Carrera et al.*, 2006]. Similar inferences were made for fold interference structures in the Atlas Mountains of

northern Africa [*Beauchamp*, 2004]. The coincidence in the central Andes of the GPS deformation pattern with the overall shape and geologic strain field [*Gephart*, 1994; *Hindle et al.*, 2002; *Allmendinger et al.*, 2005] gives no clue to a major reorganization of the regional stress or strain fields in Cenozoic time and neither do plate tectonic reconstructions [*Somoza*, 1998]. This makes the second alternative look attractive, but despite some remarks on the kinematics we made in an earlier paper [*Kley et al.*, 2005], no thorough kinematic or dynamic analysis of the phenomenon has apparently been made, either for the Salta rift or for other examples. Centrifuged plasticine-silicone models have produced pronounced contraction structures transverse to tear faults and perpendicular to the transport direction [*Dixon and Spratt*, 2004], but these appear to result from gravitational collapse and are not observed in the natural examples shown in the same paper. More structural and kinematic data from detailed case studies will be necessary to resolve this issue, which has major implications for the interpretation of noncoaxial folding in general.

5. Conclusions

[53] The Tres Cruces synclinorium in the Eastern Cordillera of northern Argentina is an inverted segment of the Tres Cruces basin, a subbasin of the Cretaceous Salta group rift. Despite strong Cenozoic folding and thrusting, some extensional structures are preserved practically unmodified and excellently exposed. The most remarkable structures are half grabens filled by synrift growth strata along the eastern border of the synclinorium. The synrift strata thicken and diverge toward the east-striking, south-dipping listric normal faults that were active during their deposition, forming rollover anticlines in their hanging walls. The stratigraphic relationships between the synrift deposits of neighboring half grabens indicate a south-to-north propagation direction of faulting, corresponding to a fault nucleation sequence into the footwall. The dynamics of faulting controlled progradational and retrogradational processes in the synrift deposits as evidenced by onlapping and offlapping stratal patterns. Combined with the progressive tilting during ongoing extension this produced internal unconformities in the synrift strata. Although the largest half-graben structure strongly resembles ideal listric fault models, geometric modeling suggests it had a more complex evolution including a gentle synclinal depression of the footwall and probably a late downcutting of the basal detachment that left the original detachment inactive. Monoclines are observed in the postrift succession above the tip lines of some normal faults. These monoclines presumably formed as extensional fault-propagation folds during a late, weak extensional reactivation that occurred in the postrift phase. They may have been amplified by differential compaction of the synrift strata whose thicknesses vary notably across the major faults, and some of them further tightened because of mild Cenozoic shortening.

[54] The system of preserved normal faults strikes east, perpendicular to the north trend of the Tres Cruces subbasin and presumably also perpendicular to approximately north-striking, longitudinal master faults. We therefore interpret the majority of the east-trending faults to be release faults [*Destro*, 1995], caused by differential displacement on the rift-parallel longitudinal faults.

[55] The evidence for normal fault rectivation in the Tres Cruces synclinorium is more circumstantial, because mostly postrift and younger strata are exposed. Yet the unusual geometries of broad, dome-shaped anticlines with spur-like extensions of lesser wavelength suggest the inversion of half grabens of approximately triangular map view shape that formed at the intersections of north- and east-trending normal faults of approximately triangular shape in map view.

[56] A compilation of the normal faults analyzed in this paper and other examples from publications on the Salta rift suggests three main controls on reverse reactivation: dip angle, strike direction, and downdip fault curvature. A dip angle less than approximately 60° was apparently required for the reactivation of faults that strike roughly orthogonal (approximately 90–60°) to the contraction direction. Faults at lower strike angles (approximately 60–30°) were reactivated at steeper dips at least sometimes with increasing strike-slip components. Fault preservation is favored at strike angles lower than approximately 30° very likely owing to the decreasing shear stress on the preexisting fault plane. Reactivation was apparently facilitated by larger radii of downdip fault curvature, indicating an influence of either the work required to bend the hanging wall as it moved up the listric fault or of detachment strength which may have been depth dependent.

[57] An intriguing problem is presented by a few reactivated normal faults striking east, with fault kinematic data indicating N-S contraction. While it appears unlikely that this reflects a regional (orogen-scale) stress field reorganization, so far no consistent models exist to convincingly explain how these structures might have formed as a side effect to east-directed shortening, even if preexisting structures are involved.

[58] **Acknowledgments.** C.R. Monaldi and J.A. Salfity were supported by the grants PIP-CONICET 02827 and CIUNSa 1456; J. Kley was supported through Deutsche Forschungsgemeinschaft (DFG) grant Kl 495/8-1. Enrique López expertly drafted most of the figures. Stereograms were created with R. W. Allmendinger's StereoWin program. Suggestions by Andrés Folguera, an anonymous reviewer, and the editor O. Oncken helped us to substantially improve the scope and focus of this paper.

References

Allmendinger, R. W. (1998), Inverse and forward numerical modeling of trishear fault-propagation folds, *Tectonics*, *17*(4), 640–656.

Allmendinger, R. W., R. Smalley, M. Bevis, H. Caprio, and B. Brooks (2005), Bending the Bolivian orocline in real time, *Geology*, *33*, 905–908.

Amengual, R., and J. C. Zanettini (1973), Geología de la comarca de Cianzo y Caspalá (Provincia de Jujuy), *Rev. Asoc. Geol. Argent.*, *28*, 341–352.

Beauchamp, W. (2004), Superposed folding resulting from inversion of a synrift accommodation zone, Atlas mountains, Morocco, in *Thrust Tectonics and Hydrocarbon Systems*, *AAPG Mem. Ser.*, vol. 82, pp. 635–646, edited by K. R. McClay, AAPG, Tulsa, Okla.

Bianucci, H. A. (1999), Estructura y evolución estructural del rift-relación con la estratigrafía: Subcuenca de Lomas de Olmedo (rama oriental), in *Geología del*

Noroeste Argentino: Relatorio del 14th Congreso Geologico Argentino, Salta 1999, tomo 1, edited by G. González Bonorino, R. Omarini and J. Viramonte, pp. 292–300, Univ. Nac. de Salta, Salta, Argentina.

Bianucci, H. A., and J. F. Homovc (1982), Tectogénesis de un sector de la cuenca del Subgrupo Pirgua, noroeste argentino, paper presented at 5th Congreso Latinoamericano de Geología, Serv. Geol. Nac., Buenos Aires.

Bianucci, H. A., J. F. Homovc, and O. M. Acevedo (1982), Inversión tectónica y plegamientos resultantes en la comarca Puesto Guardián-Dos Puntitas, Dpto. Orán, provincia de Salta, paper presented at Primer Congreso Nacional de Hidrocarburos, Inst. Argentino del Petróleo y del Gas, Buenos Aires.

Boll, A., and M. Hernández (1986), Interpretación estructural del área Tres Cruces, *Bol. Inf. Pet.*, *7*, 2–14.

Brun, J.-P., and T. Nalpas (1996), Graben inversion in nature and experiments, *Tectonics*, *15*(3), 677–687.

Buiter, S. J. H., and O. A. Pfiffner (2003), Numerical models of the inversion of half-graben basins, *Tectonics*, *22*(5), 1057, doi:10.1029/2002TC001417.

Carrapa, B., D. Adelmann, G. E. Hilley, E. Mortimer, E. R. Sobel, and M. R. Strecker (2005), Oligocene range uplift and development of plateau morphology in the southern central Andes, *Tectonics*, *24*, TC4011, doi:10.1029/2004TC001762.

Carrera, N., J. A. Muñoz, F. Sàbat, R. Mon, and E. Roca (2006), The role of inversion tectonics in the structure of the Cordillera Oriental (NW Argentinian Andes), *J. Struct. Geol.*, *28*, 1921–1932.

Chiarenza, D. G., and E. Ponzoni (1989), Contribución al conocimiento geológico de la Cuenca Cretácica en el ámbito oriental de la Subcuenca de Olmedo, provincia de Salta, paper presented at Primer Congreso Nacional de la Exploración Hidrocarburos, Inst. Argentino del Petróleo y del Gas, Mar del Plata, Argentina.

Coira, B. L. (1979), Descripción geológica de la Hoja 3c, Abra Pampa, Provincia de Jujuy, *Bol. Serv. Geol. Nac. Argent.*, *170*, 1–90.

Comínguez, A. H., and V. A. Ramos (1995), Geometry and seismic expression of the Cretaceous Salta rift of northwestern Argentina, in *Petroleum Basins of South America*, *AAPG Mem. Ser.*, vol. 62, edited by A. J. Tankard, R. Suárez Soruco, and H. J. Welsink, pp. 325–340, AAPG, Tulsa, Okla.

Coutand, I., P. R. Cobbold, M. de Urreiztieta, P. Gautier, A. Chauvin, D. Gapais, E. A. Rossello, and O. López-Gamundí (2001), Style and history of Andean deformation, Puna plateau, northwestern Argentina, *Tectonics*, *20*(2), 210–234.

Cristallini, E., A. H. Cominguez, and V. A. Ramos (1997), Deep structures of the Metán-Guachipas region: Tectonic inversion in northwestern Argentina, *J. S. Am. Earth Sci.*, *10*, 403–421.

Davison, I. (1986), Listric normal faults profiles: Calculation using bed length balance and fault displacement, *J. Struct. Geol.*, *8*, 209–210.

Destro, N. (1995), Release fault: A variety of cross fault in linked extensional fault systems, in the Sergipe-Alagoas Basin, NE Brazil, *J. Struct. Geol.*, *17*, 615–629.

Dixon, J. M., and D. A. Spratt (2004), Deformation at lateral ramps and tear faults-centrifuge models and examples from the Canadian Rocky Mountains Foothills, in *Thrust Tectonics and Hydrocarbon Systems*, *AAPG Mem. Ser.*, vol. 82, edited by K. R. McClay, pp. 239–258, AAPG, Tulsa, Okla.

Dula, W. F. (1991), Geometric models of listric normal faults and rollover folds, *AAPG Bull.*, *75*, 1609–1625.

Erslev, E. A. (1991), Trishear fault-propagation folding, *Geology*, *19*, 617–620.

Galliski, M. A., and J. G. Viramonte (1988), The Cretaceous paleorift in northwestern Argentina: A petrologic approach, *J. S. Am. Earth Sci.*, *1*, 329–342.

Gangui, A. (1998), A combined structural interpretation based on seismic data and 3-D gravity modeling in the Northern Puna/Eastern Cordillera, Argentina, *Berl. Geowiss. Abh. Reihe B*, *27*, 1–127.

Gangui, A., and H.-J. Götze (1996), The deep structure of the northern Puna, Argentina: Constraints from 2-D seismic data and 3-D gravity modeling, paper presented at 13th Congreso Geológico Argentino and 3rd Congreso Nacional de la Exploración Hidrocarburos, Asociación Geol. Argentina and Inst. Argentino del Petróleo y del Gas, Buenos Aires.

Gephart, J. W. (1994), Topography and subduction geometry in the central Andes: Clues to the mechanics of a noncollisional orogen, *J. Geophys. Res.*, *99*(B6), 12,279–12,288.

Gibbs, A. D. (1983), Balanced cross-section construction from seismic sections in areas of extensional tectonics, *J. Struct. Geol.*, *5*, 153–160.

Gibbs, A. D. (1984), Structural evolution of extensional basin margins, *J. Geol. Soc. London*, *141*, 609–620.

Grier, M. (1990), The influence of the Cretaceous Salta rift basin on the development of Andean structural geometries, NW Argentine Andes, Ph. D. thesis, 178 pp., Cornell Univ., Ithaca, N. Y.

Grier, M., J. A. Salfity, and R. W. Allmendinger (1991), Andean reactivation of the Cretaceous Salta rift, northwestern Argentina, *J. S. Am. Earth Sci.*, *4*, 351–372.

Halpern, M., and C. O. Latorre (1973), Estudio geocronológico inicial de las rocas del Noroeste de la República Argentina, *Rev. Asoc. Geol. Argent.*, *28*, 196–205.

Hamblin, W. K. (1965), Origin of "reverse drag" on the downthrown side of normal faults, *Geol. Soc. Am. Bull.*, *76*, 1145–1164.

Harding, T. P. (1984), Graben hydrocarbon ocurrences and structural style, *AAPG Bull.*, *68*, 333–362.

Hauge, T. A., and G. G. Gray (1996), A critique of techniques for modelling normal-fault and rollover geometries, in *Modern Developments in Structutural Interpretation, Validation, and Modelling*, *Geol. Soc. Spec. Publ.*, vol. 99, edited by P. G. Buchanan and D. A. Nieuwland, pp. 89–97, Geol. Soc., London.

Hernández, R. M., A. Disalvo, A. Boll, R. Gómez Omil, and C. Galli (1999), Estratigrafía secuencial del Grupo Salta, con énfasis en las subcuencas de Metán-Alemania, noroeste argentino, in *Geología del Noroeste Argentino: Relatorio del 14th Congreso Geologico Argentino, Salta 1999*, tomo 1, edited by G. González Bonorino, R. Omarini, and J. Viramonte, pp. 263–283, Univ. Nac. de Salta, Salta, Argentina.

Hindle, D., J. Kley, E. Klosko, S. Stein, T. Dixon, and E. Norabuena (2002), Consistency of geologic and geodetic displacements during Andean orogenesis, *Geophys. Res. Lett.*, *29*(8), 1188, doi:10.1029/2001GL013757.

Hongn, F., C. Del Papa, J. Powell, I. Petrinovic, R. Mon, and V. Deraco (2007), Middle Eocene deformation and sedimentation in the Puna-Eastern Cordillera transition (23°–26°S): Control by preexisting heterogeneities on the pattern of initial Andean shortening, *Geology*, *35*, 271–274.

Kley, J., and C. R. Monaldi (2002), Tectonic inversion in the Santa Barbara System of the central Andean foreland thrust belt, northwestern Argentina, *Tectonics*, *21*(6), 1061, doi:10.1029/2002TC902003.

Kley, J., E. A. Rossello, C. R. Monaldi, and B. Habighorst (2005), Seismic and field evidence of Cretaceous normal faults, Salta rift, Northwest Argentina, *Tectonophysics*, *399*, 155–172.

Kress, P. (1995), Tectonic inversion of the subandean foreland: A combined geophysical and geological approach, *Berl. Geowiss. Abh. Reihe B*, *23*, 1–120.

Letouzey, J. (1986), Cenozoic paleo-stress pattern in the Alpine Foreland and structural interpretation in a platform basin, *Tectonophysics*, *132*, 215–231.

Mackin, J. H. (1950), The down-structure method of viewing geologic maps, *J. Geol.*, *58*, 55–72.

Marquillas, R. A., C. del Papa, and I. F. Sabino (2005), Sedimentary aspects and paleoenvironmental evolution of a rift basin: Salta Group (Cretaceous-Paleogene), northwestern Argentina, *Int. J. Earth Sci.*, *94*, 94–113.

Marrett, R., and M. R. Strecker (2000), Response of intracontinental deformation in the central Andes to late Cenozoic reorganization of South American Plate motions, *Tectonics*, *19*(3), 452–467.

Marrett, R., R. W. Allmendinger, R. N. Alonso, and R. E. Drake (1994), Late Cenozoic tectonic evolution of the Puna Plateau and adjacent foreland, northwestern Argentine Andes, *J. S. Am. Earth Sci.*, *7*, 179–207.

McClay, K. R., and P. G. Ellis (1987), Geometries of extensional faults developed in model experiments, *Geology*, *15*, 341–344.

Méndez, V. (1973), Geología de la comarca de Mina Aguilar y alrededores, Departamento Humahuaca (Provincia de Jujuy), *Rev. Asoc. Geol. Argent.*, *28*, 319–340.

Menegatti, N., R. Omarini, A. Del Moro, and R. Mazzuoli (1997), El granito alcalino de la sierra de Rangel (Cretácico Inferior), provincia de Salta, Argentina, paper presented at 8th Congreso Geológico Chileno, Univ. Católica del Norte, Antofagasta, Chile.

Mitra, S. (1993), Geometry and kinematic evolution of inversion structures, *AAPG Bull.*, *77*, 1159–1191.

Mon, R., C. R. Monaldi, and J. A. Salfity (2004), Interferencia de pliegues en el valle del río Juramento–Cordillera Oriental (provincia de Salta), *Rev. Asoc. Geol. Argent.*, *59*, 213–219.

Moreno, J. A. (1970), Estratigrafía y paleogeografía del Cretácico Superior en la cuenca del Noroeste Argentino, con especial mención de los Subgrupos Balbuena y Santa Bárbara, *Rev. Asoc. Geol. Argent.*, *24*, 9–44.

Morley, C. K., R. A. Nelson, T. L. Patton, and S. G. Munn (1990), Transfer zones in the East African Rift System and their relevance to hydrocarbon exploration in rifts, *AAPG Bull.*, *74*, 1234–1253.

Morrow, C. A., L. Q. Shi, and J. D. Byerlee (1982), Strain hardening and strength of clay-rich fault gouges, *J. Geophys. Res.*, *87*(B8), 6771–6780.

Panien, M., G. Schreurs, and A. Pfiffner (2005), Sandbox experiments on basin inversion: Testing the influence of basin orientation and basin fill, *J. Struct. Geol.*, *27*, 433–445.

Pardo-Casas, F., and P. Molnar (1987), Relative motion of the Nazca (Farallon) and South American plates since Late Cretaceous time, *Tectonics*, *6*, 233–248.

Reyes, F. C. (1972), Correlaciones en el Cretácico de la cuenca Andina de Bolivia, Perú y Chile, *Rev. Téc. YPFB*, *1*, 101–144.

Reyes, F. C., and J. A. Salfity (1973), Consideraciones sobre la estratigrafía del Cretácico (Subgrupo Pirgua) del noroeste argentino, paper presented at 5th Congreso Geológico Argentino, Asociación Geol. Argentina, Buenos Aires.

Reynolds, J., C. Galli, R. Hernández, B. Idleman, J. M. Kotila, R. V. Hilliard, and C. W. Naeser (2000), Middle Miocene tectonic developmentof the transition zone, Salta Province, northwest Argentina: Magnetic stratigraphy from the Metán Subgroup, Sierra de González, *Geol. Soc. Am. Bull.*, *112*, 1736–1751.

Salfity, J. A., and R. A. Marquillas (1994), Tectonic and sedimentary evolution of the Cretaceous-Eocene Salta Group basin, Argentina, in *Cretaceous Tectonics of the Andes*, edited by J. A. Salfity, pp. 266–315, Vieweg Verlag, Wiesbaden, Germany.

Salfity, J. A., C. R. Monaldi, R. A. Marquillas, and R. E. González (1993), La inversión tectónica del Umbral de Los Gallos en la cuenca del Grupo Salta durante la Fase Incaica, paper presented at 12th Congreso Geológico Argentino and 2nd Congreso Nacional de la Exploración Hidrocarburos, Asociación Geol. Argentina and Inst. Argentino del Petróleo y del Gas, Mendoza, Argentina.

Shaw, J. H., S. C. Hook, and E. P. Sitohang (1997), Extensional fault-bend folding and synrift deposition: An example from the Central Sumatra Basin, Indonesia, *AAPG Bull.*, *81*, 367–379.

Sibson, R. H. (1995), Selective fault reactivation during basin inversion: Potential for fluid redistribution

through fault-valve action, in *Basin Inversion*, *Geol. Soc. Spec. Publ.*, vol. 88, edited by J. G. Buchanan and P. G. Buchanan, pp. 3–19, Geol. Soc., London.

Sibson, R. H. (2004), Frictional mechanics of seismogenics thrust systems in the upper continental crust: Implications for fluid overpressures and redistribution, in *Thrust Tectonics and Hydrocarbon Systems*, *AAPG Mem. Ser.*, vol. 82, edited by K. R. McClay, pp. 1–17, AAPG, Tulsa, Okla.

Skuce, A. G. (1996), Forward modelling of compaction above normal faults: An example from the Sirte Basin, Libya, in *Modern Developments in Structutural Interpretation, Validation, and Modelling*, *Geol. Soc. Spec. Publ.*, vol. 99, edited by P. G. Buchanan and D. A. Nieuwland, pp. 135–146, Geol. Soc., London.

Somoza, R. (1998), Updated Nazca (Farallon)-South America relative motions during the last 40 My: Implications for mountain building in the Central Andean region, *J. S. Am. Earth Sci.*, *11*, 211–215.

Starck, D. (1995), Silurian-Jurassic stratigraphy and basin evolution of northwestern Argentina, in *Petroleum Basins of South America*, *AAPG Mem. Ser.*, vol. 62, edited by A. J. Tankard, R. Suárez Soruco, and H. J. Welsink, pp. 251–267, AAPG, Tulsa, Okla.

Stearns, D. W. (1978), Faulting and forced folding in the Rocky Mountains foreland, *Geol. Soc. Am. Bull.*, *151*, 1–38.

Strecker, M. R., and R. Marrett (1999), Kinematic evolution of fault ramps and its role in development of landslides and lakes in the northwestern Argentine Andes, *Geology*, *27*, 307–310.

Suppe, J., and D. A. Medwedeff (1990), Geometry and kinematics of fault-propagation folding, *Eclogae Geol. Helv.*, *83*, 409–453.

Uliana, M. A., and K. T. Biddle (1988), Mesozoic-Cenozoic paleogeographic and geodynamic evolution of southern South America, *Rev. Bras. Geocienc.*, *18*, 172–190.

Uliana, M. A., M. E. Arteaga, L. Legarreta, J. J. Cerdán, and G. O. Peroni (1995), Inversion structures and hydrocarbon occurrence in Argentina, in *Basin Inversion*, *Geol. Soc. Spec. Publ.*, vol. 88, edited by J. G. Buchanan and P. G. Buchanan, pp. 211–233, Geol. Soc., London.

Viramonte, J. G., S. M. Kay, R. Becchio, M. Escayola, and I. Novitski (1999), Cretaceous rift related magmatism in central-western South America, *J. S. Am. Earth Sci.*, *12*, 109–121.

Wang, G. M., M. P. Coward, W. Yuan, S. Liu, and W. Wang (1995), Fold growth during basin inversion: Example from the East China Sea Basin, in *Basin Inversion*, *Geol. Soc. Spec. Publ.*, vol. 88, edited by J. G. Buchanan and P. G. Buchanan, pp. 493–522, Geol. Soc., London.

White, N. J., J. A. Jackson, and D. P. Mc Kenzie (1986), The relationship between the geometry of normal faults and that of sedimentary layers in the hanging walls, *J. Struct. Geol.*, *8*, 897–910.

Williams, G., and I. Vann (1987), The geometry of listric normal faults and deformation in their hanging walls, *J. Struct. Geol.*, *9*, 789–795.

Withjack, M. O., Q. T. Islam, and P. R. La Pointe (1995), Normal faults and their hanging-wall deformation: An experimental study, *AAPG Bull.*, *79*, 1–18.

Xiao, H., and J. Suppe (1992), Origin of rollover, *AAPG Bull*, *76*, 509–525.

Jonas Kley, Institut für Geowissenschaften, Friedrich-Schiller-Universität Jena, Burgweg 11, D-07749 Jena, Germany.

C. R. Monaldi and J. A. Salfity, Consejo Nacional de Investigaciones Científicas y Técnicas, Universidad Nacional de Salta, Buenos Aires 177, 4400 Salta, Argentina. (crmonaldi@arnet.com.ar)